SOME ASPECTS OF THE ATMOSPHERIC ELECTRIC CLIMATE AT IBADAN

By

DEBORAH OLUSEUN ADEWOLU
B.Sc. Hons. (Ibadan)

A Thesis in the Department of Physics
Submitted to the Faculty of Science

In Partial Fulfilment of The
Requirements For The Degree Of

MASTER OF PHILOSOPHY

Of The

UNIVERSITY OF IBADAN

July, 1980

ABSTRACT

The diurnal variations of the atmospheric electric parameters and meteorological parameters for the harmattan season of November 1978 to March 1979 are presented.

The percentage variations of temperature are mirror images of those of vapour pressure which show pronounced depressions around noon when the little available moisture in the air near the ground is distributed over greater and greater heights by convection.

The diurnal patterns of dust concentration, measured for the first time in this locality, is single periodic with minimum between 0400 hrs and 0800 hrs L.T. and maximum around 20 hrs L.T. This pattern is closely related to that of windspeed, and is explained in terms of the copious amount of dust transported southwards from the Sahara desert.

The diurnal curves of the electric elements, I, H and ρ show pronounced "austausch" depressions around noon and marked peaks at 08.00 hrs which are attributable to the sunrise effect.

An average value of the total nuclei concentration during the Harmattan months is computed to be about 2.8×10^{10} particles per m^3 for this station. This value is based on the measurements of the polar conductivities made for the first time in Ibadan.

ACKNOWLEDGEMENTS

C E R T I F I C A T I O N

This is to certify that this work was carried out by Miss DEBORAH OLUSEUN ADEWOLU in the Department of Physics, University of Ibadan.

(signature)

A.I.I Ette, B.Sc., Ph.D. (London)
Professor in the Department of
Physics, University of Ibadan,
Nigeria.

July 1980.

TABLE OF CONTENTS

INDEX OF FIGURES

CHAPTER I

1.1. INTRODUCTION

Atmospheric electricity, the systematic study of electrical properties of the earths gaseous envelope, dates back to 1708 when Wall speculated that the phenomenon of lightning was similar to electrical discharge in the laboratory. This surmise was later verified independently in 1752 D'alibard and Franklin.

Lemonnier (1752) observed that the atmosphere is the seat of electric field even in fine weather. Using an arrangement of an elevated, insulated, horizontally stretched wire - first introduced by Lemonnier, Beccaria (1775) measured the potential gradient on a continuous basis. He found that during fine weather the potential gradient is predominantly positive and has a definite diurnal pattern.

The pattern of variation of the potential gradient and of other atmospheric electric parameters is controlled by meteorological and aerological factors, and so one can talk of the atmospheric electric climate at a station.

- 10 -

1.2. THE SPHERICAL CAPACITOR CONCEPT

Owing to ionization of the air by cosmic rays and radio-
active emanations from the earth's crust, the atmosphere has
a conductivity profile which increases rapidly with height.
At a height of about 50km the conductivity of the atmosphere
is comparable to that of the earth's crust, so that the
atmosphere may be considered as confined between two highly
conducting spheres - the outer one of which is usually called
the equalizing layer or the electrosphere (vide Fig. 1).
This spherical capacitor concept of the atmosphere is
attributed to Kelvin (1860); though as early as 1751, Watson,
from analogy with laboratory experiments involving electrical
discharge in rarefied gases, had suggested an increase in the
conductivity of the atmosphere with height.

Gish (1951) has estimated that during fine weather a
total leakage current of 1,800A flows through an effective
resistance of 200 Ω from the electrosphere to earth. This
indicates an average electrosphere potential of +360,000V
relative to earth. More recent estimates based on the data
obtained by Muhleisen (1971) suggest a lower leakage current
of about 665A and an average electrosphere potential of
+250,000V.
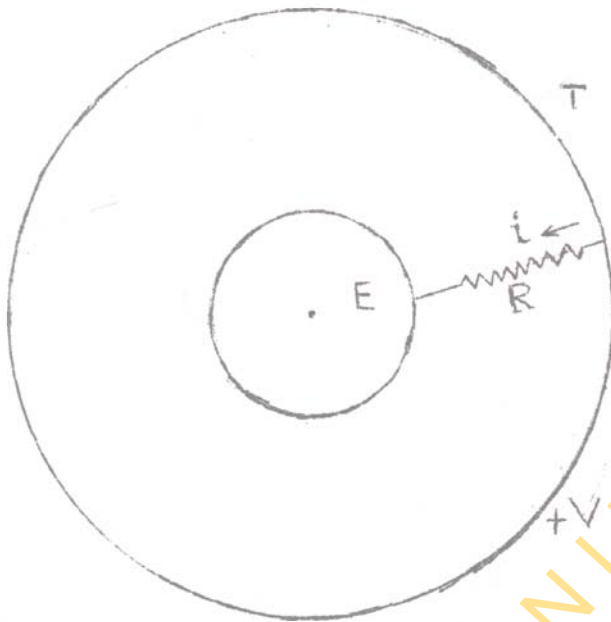
Fig. 1:   The spherical Capacitor picture of the atmosphere.

1.3.   THE CLASSICAL PICTURE

It is clear that a spherical capacitor with a leaky dielectric, such as depicted in Fig. 1, cannot give rise to a persistent electric field. Kasemir (1950) has shown that such a system would be completely discharged in about 30 minutes. The fact that this does not happen in practice points to the existence of a charging mechanism in the atmosphere. Wilson (1920) suggested that this mechanism is geared to the charge generators in thunderstorm clouds.

The coupling of these generators to the atmospheric capacitor gave rise to the classical picture of atmospheric electricity (Fig. 2). Evidence in support of this picture has been provided by Whipple and Scrase (1936), Mühleisen (1971), and Ette and Uttah (1973). However, Lobodin (1968) and Webb (1971) have argued that global thunderstorm activity plays an insignificant role in the electrification of the atmospheric capacitor, though there is so far no strong experimental evidence in support of their views.
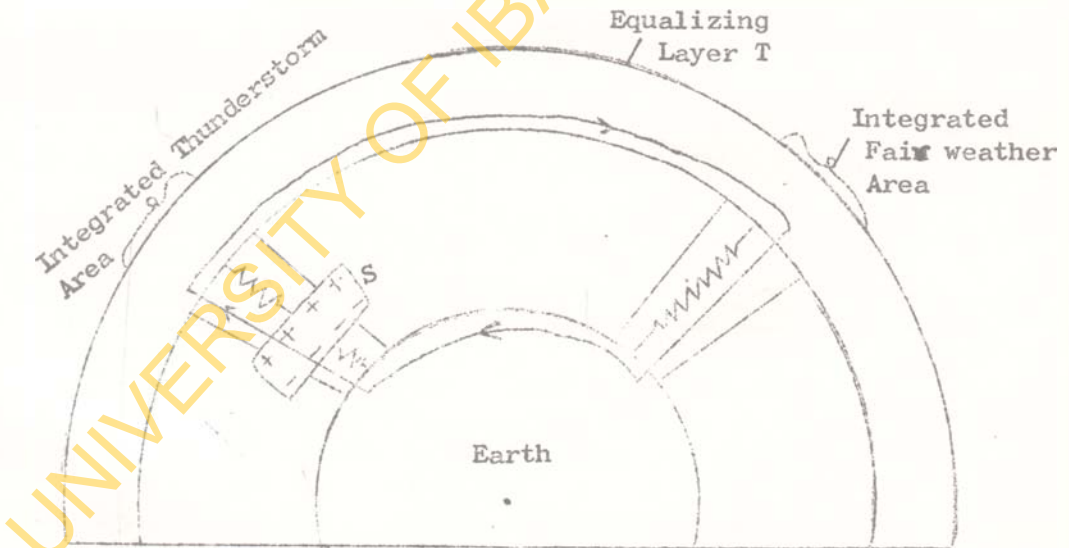
Fig. 2: <u>The classical picture of the atmosphere</u>. Arrows show the direction of flow of current between the integrated thunderstorm and fair-weather areas.

1.4. COMPOSITION OF THE ATMOSPHERE

The gaseous composition of a typical atmosphere is
given in Table 1:

Table 1:

Constituent	% by Volume	% by Mass
Nitrogen	78.09	75.51
Oxygen	20.95	23.14
Argon	0.93	1.3
Carbondioxide (variable)	0.03	0.05
Neon	180×10^{-5}	120×10^{-5}
Helium	52×10^{-5}	8×10^{-5}
Krypton	10×10^{-5}	29×10^{-5}
Hydrogen	5×10^{-5}	0.35×10^{-5}
Xenon	0.8×10^{-5}	3.6×10^{-5}
Ozone (variable)	0.1×10^{-5}	0.17×10^{-5}
Water vapour (variable)		

There are also traces of carbon monoxide, radon,
nitrous oxide and methane. The non-gaseous constituents of
the atmosphere are dust, smoke, salt particles from the
evaporation of sea sprays (aerosols) and condensed water,
ice, hail and snow (hydrometeors). The concentrations of
these constituents are highly variable. It is in fact the
variable components of the atmosphere which largely
determine the meteorological and electrical state of the

atmosphere. In particular, the impact of convection -
leading to a vertical exchange of physical properties or
"austausch" - is crucial in modifying the patterns of
variation of the atmospheric electric parameters at a
station.

1.5. THE FAIR-WEATHER ATMOSPHERE

In   fair weather the atmosphere is characterized by

(a) absence of pollution or hydrometeors,

(b) little or no cloud cover, and

(c) windspeeds less than $6ms^{-1}$.

Under these conditions, the atmospheric electric parameters
vary rather slowly with time; and the atmospheric impedance
may be taken as purely resistive. A small vertical portion
of such an atmosphere may thus be represented as in Fig. 3.
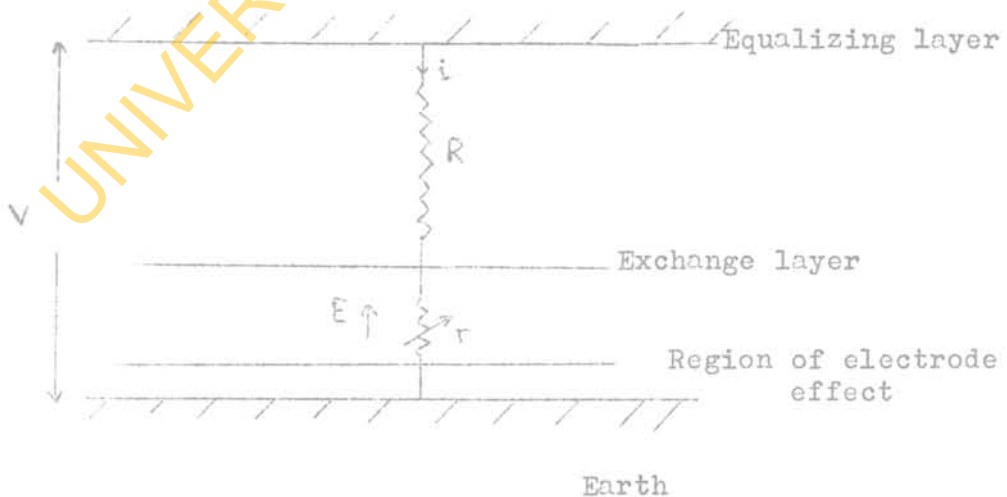
Fig. 3: Electrical Structure of the fair weather atmosphere.

R = total columnar resistance (Ω)

V = potential of equalizing layer (V)

i = conduction current density (Am^{-2})

E = potential gradient (Vm^{-1})

r = specific columnar resistance (Ωm^{-1})

In this diagram the total columnar resistance R is the resistance of a column of air of unit cross sectional area extending from the earth to the equalizing layer. The resistance of a unit length of this column is the specific columnar resistance r. The conduction current flowing into a unit cross-sectional area is the current density i. The flow of this current through the resistance r produces a vertical potential difference represented by E, the vertical potential gradient.

In fair-weather the current density i has the same value at all heights, though all the other parameters vary with height.

The exchange layer is the region of vigorous vertical exchange or "austausch", within which meteorological and electrical characteristics undergo the greatest diurnal variations. The layer varies in height between about 0.1 to 3km, depending on locality and season.

Close to the ground is the region of electrode effect, where, on account of the predominance of ions of one sign

moving into the earth electrode, the various electrical
parameters, such as conductivity, space-charge density etc.
are generally not representative of values in higher regions
of the exchange layer.   The height of the electrode effect
layer is typically a few meters, and is more pronounced over
oceans.

1.6.   OHM'S LAW RELATIONS

Under quasi-stationary conditions, we may apply Ohm's
law to relate the above parameters.

Thus we have

$$V = iR, \qquad \text{------------} \qquad (1.1)$$

$$E = ir; \qquad \text{------------} \qquad (1.2)$$

whence

$$E = (r/R).V \qquad \text{------------} \qquad (1.3)$$

Since

$$r = 1/\lambda = \frac{1}{(\lambda_+ + \lambda_-)} , \qquad \text{------------} \qquad (1.4)$$

where λ_+ and λ_- are the positive and negative polar
conductivities of the air, equation (1.2) can be written
alternatively as

$$i = E (\lambda_+ + \lambda_-) \qquad \text{------------} \qquad (1.5)$$

V and R cannot be measured directly, but may be deduced from vertical profiles of E and λ respectively as follows:

$$V = \int_{0}^{H} E\, dz, \quad \text{and}$$

$$R = \int_{0}^{H} \frac{dz}{\lambda},$$

$$= \int_{0}^{H} \gamma\, dz$$

where the height H corresponds to the equalizing layer; though in practice it is taken as the maximum height of baloon ascents-approximately 20km.

It follows from eqn. (1.5) that the parameter

$$\Lambda = \frac{E}{i/(\lambda_{+} + \lambda_{-})}$$, the so-called Ohm's law parameter, should be unity. Investigations by various workers (e.g. Dolezalek, 1972; Bhartendu, 1969) show however that at most stations the ratio deviates significantly from unity and fluctuates considerably. Ette (1972) has questioned the propriety of applying Ohm's law within the exchange layer where the effect of turbulence on the general aerological condition tends to set up local generators and transform the columnar impedances to active elements.

1.7. RELATIONS BETWEEN TIME VARIATIONS OF THE
ATMOSPHERIC ELECTRIC PARAMETERS

Considering quasi-stationary changes in the atmospheric electric parameters (e.g. diurnal variations) such that inductive and capacitive effects can be neglected, we have, from differentiating equations (1.1) and (1.5)

$$\frac{di}{dt} = \frac{1}{R}\frac{dv}{dt} - \frac{V}{R^2}\frac{dR}{dt} \qquad \qquad (1.6)$$

and

$$\frac{di}{dt} = E\frac{d\lambda}{dt} + \lambda\frac{dE}{dt} \qquad \qquad (1.7)$$

Dividing equation (1.6) by equation (1.1) and equation (1.7) by (1.5) gives

$$\frac{1}{i}\frac{di}{dt} = \frac{1}{V}\frac{dV}{dt} - \frac{1}{R}\frac{dR}{dt} \qquad \qquad (1.8)$$

$$\frac{1}{i}\frac{di}{dt} = \frac{1}{\lambda}\frac{d\lambda}{dt} + \frac{1}{E}\frac{dE}{dt} \qquad \qquad (1.9)$$

Eliminating $\frac{1}{i}\frac{di}{dt}$ between equations (1.8) and (1.9), we have

$$\frac{1}{E}\frac{dE}{dt} = \frac{1}{V}\frac{dV}{dt} - \frac{1}{R}\frac{dR}{dt} - \frac{1}{\lambda}\frac{d\lambda}{dt} \qquad \qquad (1.10)$$

Equations (1.8), (1.9) and (1.10) express the relations
between the percentage changes in R and V on one hand and
those of i, E and λ on the other. Thus, although R and V
are not directly measurable, their time variations can under
suitable conditions, be investigated from ground measurements
of variation of i, E and λ.

Three special cases of equations (1.8), (1.9) and (1.10)
are of particular interest. These are
Case (I) R and λ independent of time
Case (II) R independent of time and
Case (III) V independent of time.

Case I: The situation in which R and λ are constant
can only be observed where the influence of 'austausch' is
minimum. This is likely to be the case over oceans and ice
fields where temperatures tend to be fairly uniform through-
out the day. With these conditions satisfied we have, from
equations (1.8) and (1.9) putting $\frac{d\lambda}{dt} = \frac{dR}{dt} = 0$,

$$\frac{1}{I}\frac{di}{dt} = \frac{1}{E}\frac{dE}{dt} = \frac{1}{V}\frac{dV}{dt} \quad \text{—} \quad \text{—} \quad \text{—} \quad \text{—} \quad \text{—} \quad \text{—} \qquad (1.11)$$

Data obtained from the Carnegie cruise and plotted in Fig. 4
confirm that over oceans the diurnal curves for i and E are
almost identical. It may therefore be concluded that these
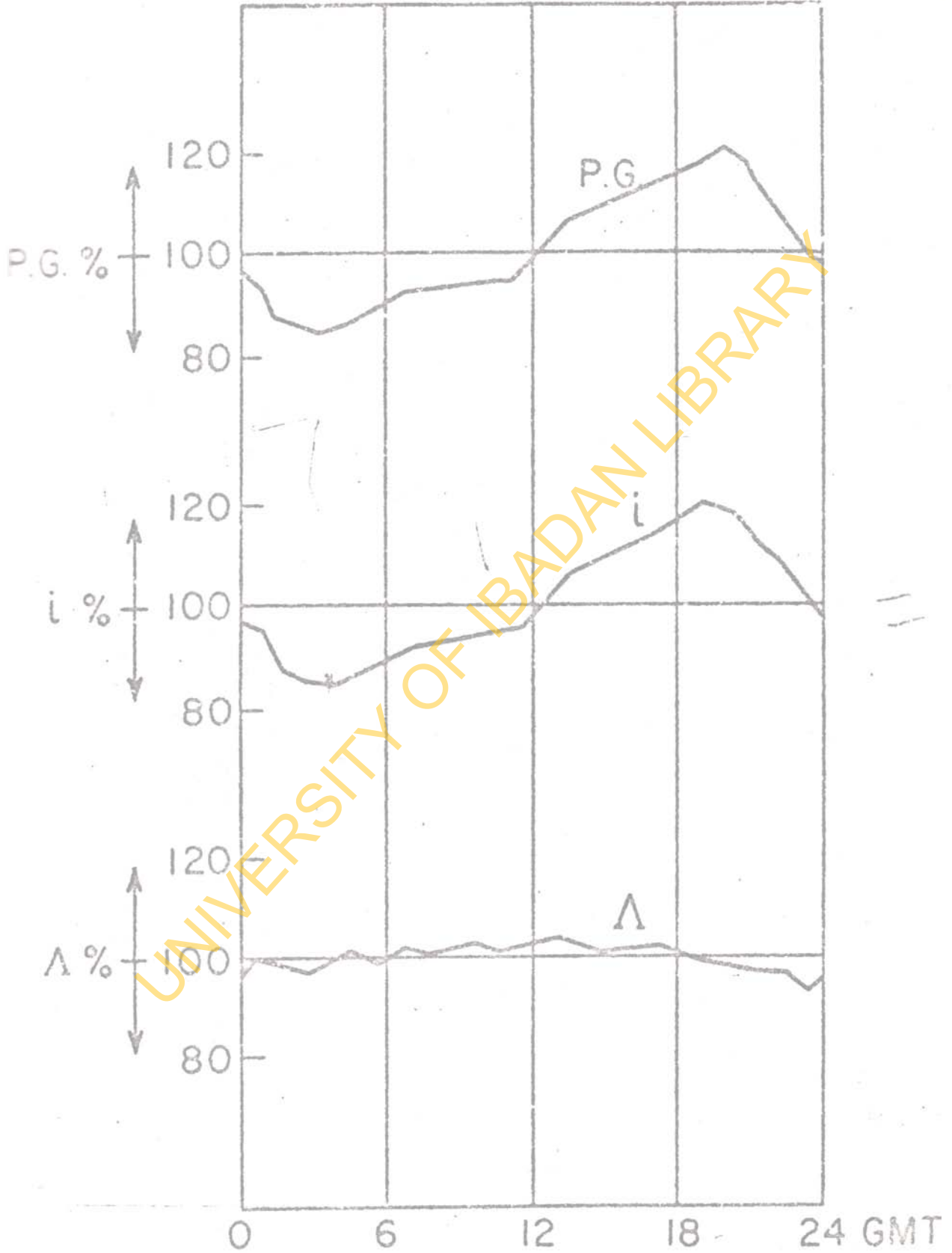
FIG 4 : E, i, Λ For OCEANS

curves also represent the diurnal variation of V, the
electrosphere potential.

Case II: With R constant, we expect, from equation
(1.8) that

$$\frac{1}{i} \frac{di}{dt} = \frac{1}{V} \frac{dV}{dt} \quad \text{--} \quad \text{--} \quad \text{--} \quad \text{--} \quad \text{--} \quad \text{--} \quad (1.12)$$

Thus, once again the diurnal variation of i should reflect
the diurnal variation of V. The situation in which R is
constant should be approximated on high mountain stations
which lie well above the exchange layer. Thus, mountain
stations, like oceans, should be globally representative.

Data presented by Israel and de Bruijn (1967) suggest
however that over mountain stations as high as 3.6km
measurements are not globally representative.

Case III: The case where V is constant at first sight
looks unrealistic, since V is known to vary with universal
time. Since however, at any instant of time V is the same
over all stations, its variation with time can be eliminated
from consideration by considering normalized currents and
potential gradients at a station and defined as

$$I = \frac{i}{i_o} = \frac{\text{Current density over land}}{\text{Simultaneous current density over oceans}} \text{ , and}$$

$$H = E/E_0 = \frac{\text{Potential gradient over land}}{\text{Simultaneous potential gradient over oceans}}$$

Thus we have

$$I = \frac{V/R}{V/R_0} = K_1 \cdot \frac{1}{R}, \qquad \text{---} \quad \text{---} \qquad \text{---} \quad \text{---} \qquad (1.13)$$

where $K_1 = R_0$, a constant; and

$$H = \frac{r}{R} \cdot V \Big/ \frac{r_0}{R_0} \cdot V = K_2 \frac{r}{R}, \qquad \text{---} \quad \text{---} \qquad \text{---} \quad \text{---} \qquad (1.14)$$

where $K_2 = \dfrac{R_0}{r_0}$, another constant.

Taking logarithms and differentiating equations (1.13) and (1.14) with respect to time, we have

$$\frac{1}{I} \frac{dI}{dt} = -\frac{1}{R} \frac{dR}{dt} \qquad \text{---} \quad \text{---} \qquad \text{---} \quad \text{---} \qquad (1.15)$$

and

$$\frac{1}{H} \frac{dH}{dt} = \frac{1}{r} \frac{dr}{dt} - \frac{1}{R} \frac{dR}{dt} \qquad \text{---} \quad \text{---} \qquad \text{---} \quad \text{---} \qquad (1.16)$$

Thus with the new parameters I and H as defined, the per-centage diurnal variation of I should give the percentage diurnal variation of R; and the percentage diurnal variation of H should reflect the difference in the percentage diurnal variations of r and R. A major advantage in the use of

equations (1.15) and (1.16) is that since percentage changes
are involved it is not essential to determine absolute values
of the measured parameters, which in any case for some of the
parameters are not always easy to measure accurately.

1.8. INFLUENCE OF METEOROLOGICAL AND AEROLOGICAL FACTORS

Two factors are commonly identified as playing signi-
ficant roles in causing deviations of the diurnal pattern of
the potential gradient at land stations from the single
periodic pattern. These are the moisture content of the
air (measured by the vapour pressure) and the aerosol
concentration. For many stations the potential gradient and
the **vapour** pressure undergo parallel variations (see Fig. 5
for Potsdam); and so both variations may be attributed to a
similar cause.

The single periodic or maritime type of variation of
vapour pressure occurs when there is enough water vapour
supply in the atmosphere through evaporation. Hence vapour
pressure variation follows temperature variation very
closely. Thus increase in temperature in the morning hours
gives rise to increase in evaporation and hence the vapour
pressure, until the peak is reached in the late afternoon.
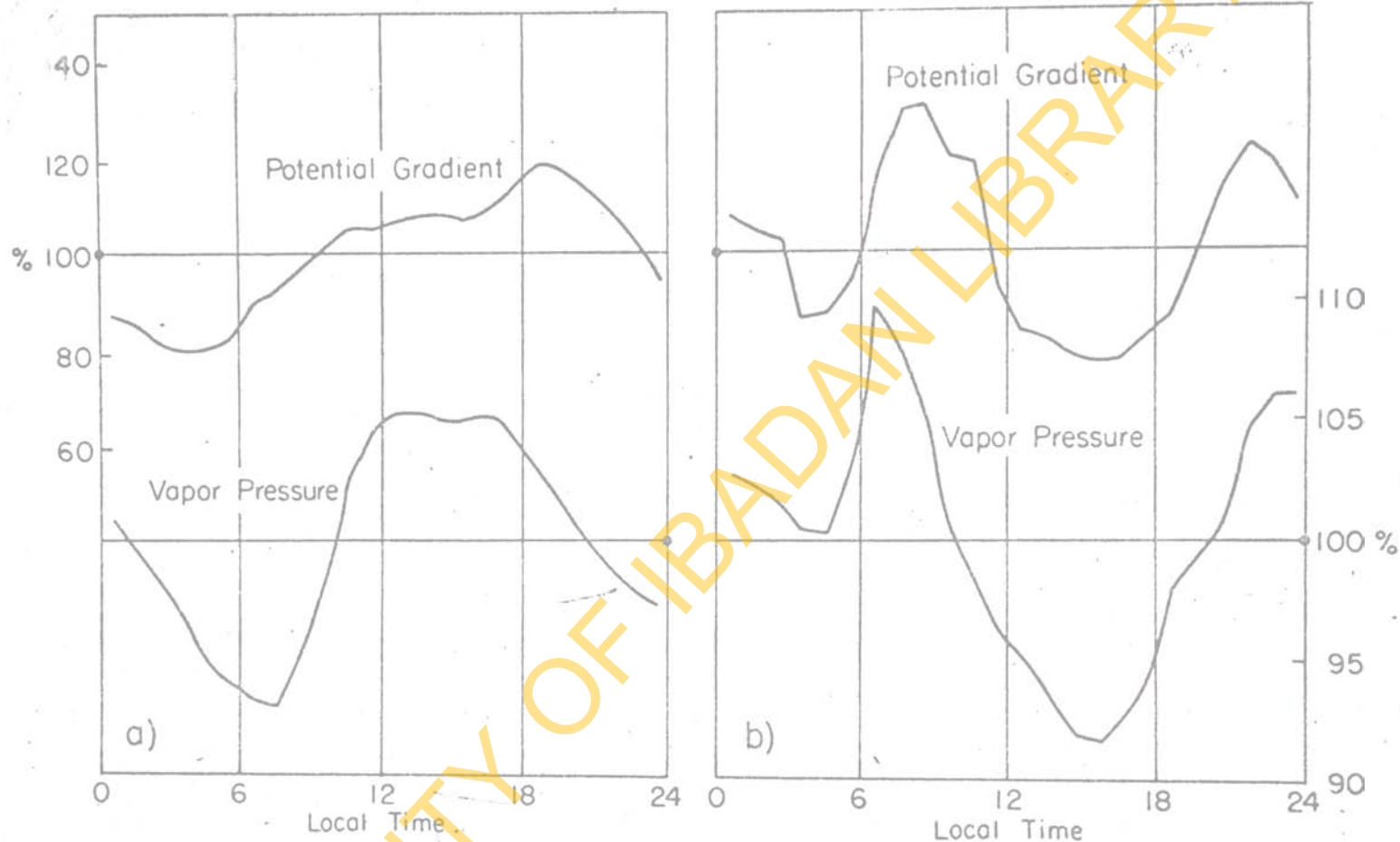
FIG. 5. — Associated variation types of potential gradient and vapor pressure in percentages (according to the recordings in Potsdam, 1934-37) (Israël, 1950).

In the evening when temperature falls, evaporation and hence
vapour pressure also decreases. At night condensation leads to
further decrease in the vapour pressure.

The double-periodic or convective type of variation in
vapour pressure is explained as due to the effect of convection
upon the simple daily variation. After sunrise, when temperature
and vapour pressure increase, convection currents also set in,
producing a mixture of the moisture rich layers near the ground
and the poorer layers higher up. This results in a reduction of
moisture content, and hence the vapour pressure in the lower
layers. This decrease continues as convection penetrates to
higher and higher layers. After convection attains its maximum
strength in late afternoon, the effect of evaporation begins to
predominate over moisture depletion near the surface; and so the
vapour pressure increases in the evening, until with decreasing
temperature saturation, and later condensation, occurs.

A similar explanation - involving the superposition of the
effect of "austausch" on the simple daily curve of production -
has been offered by Whipple (1929) to explain the double periodic
variation in aerosol concentration at land stations. For Kew near
London where a lot of pollution is generated through industrial
activity, this parameter undergoes a strickingly parallel
variation with the potential gradient (see Fig. 6).
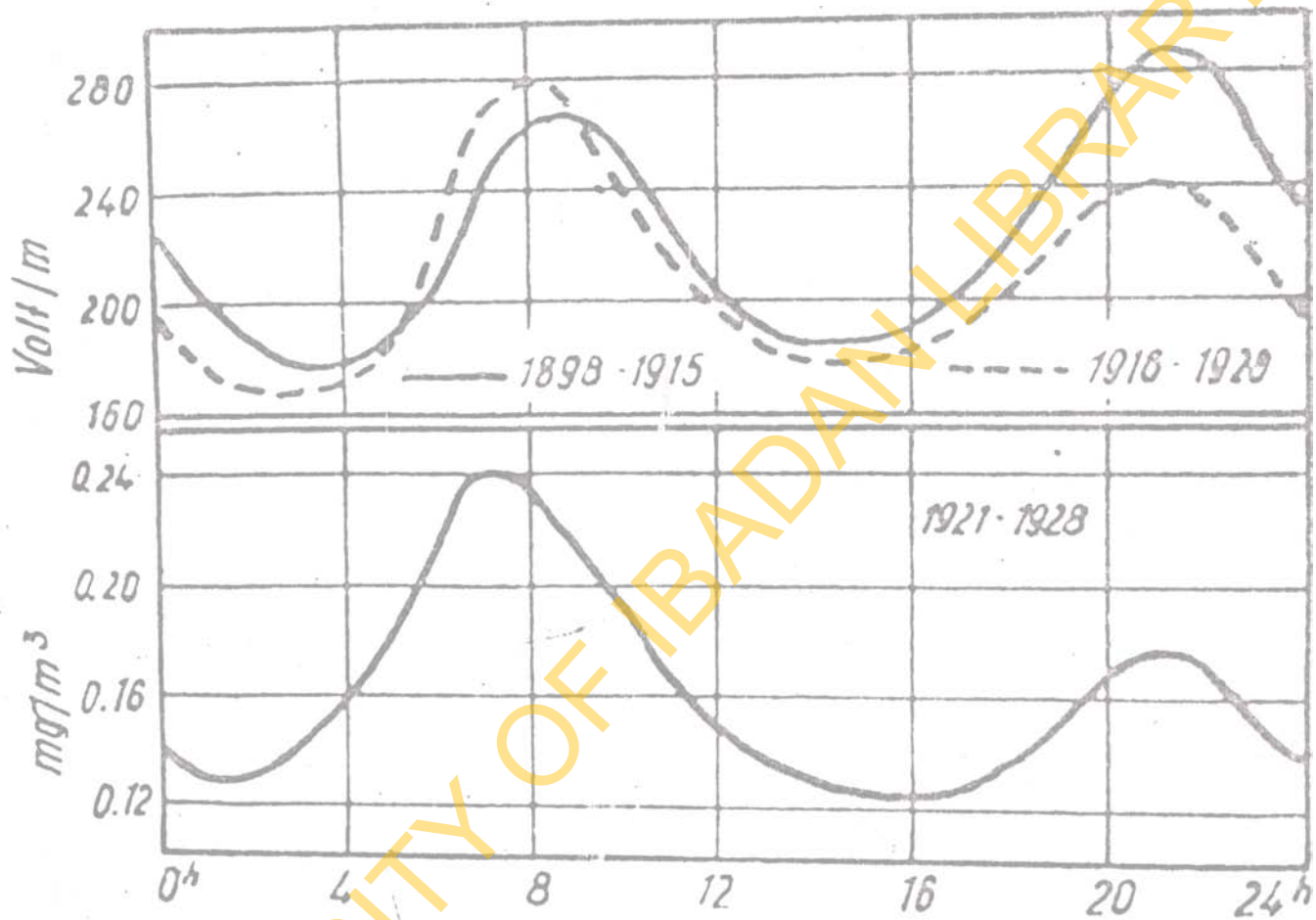
FIG 6. – Daily variation in the atmospheric electrical potential gradient and the atmospheric pollution at Kew during the summer months, according to F. J. W. Whipple (1929).

1.9. DIURNAL VARIATIONS IN ELECTRIC POTENTIAL GRADIENT E

There are two basic types of diurnal variations of
atmospheric electric potential gradient namely:

(i) the single-periodic type variation observed over
   oceans and polar ice fields, and

(ii) the double-periodic type variation characteristic of
   most non-polar continential stations.

The single-periodic type (see Fig. 4) of variation
proceeds according to universal time with a minimum occurring
at about 0400 G.M.T. and a maximum at about 1900 G.M.T.
The double-periodic type of variation on the other hand is
geared to local time: and for many stations in the temperate
region the diurnal pattern changes from the double periodic
type in the summer months to the single periodic type in
winter when the ground is covered with snow. There are non-
polar continental stations however where the pattern is
either single periodic throughout the year or double periodic
throughout (Israel 1948).

Considering equations (1.2) and (1.4), the potential
gradient can be expressed in terms of conductivity as

$$E = i/\lambda \qquad \text{---} \quad \text{---} \quad \text{---} \quad \text{---} \qquad \text{---} \quad \text{---} \quad \text{---} \qquad (1.17)$$

Differentiating (1.17) with respect to time and dividing by

equation (1.17) gives

$$\frac{1}{E}\frac{dE}{dt} = \frac{1}{i}\frac{di}{dt} - \frac{1}{\lambda}\frac{d\lambda}{dt}, \qquad \text{---} \quad \text{---} \quad \text{---} \quad \text{---} \quad \text{---} \quad (1.18)$$

Also from definition of parameter H of section 1.7, we have

$H = E/E_o$, which leads to equation (1.16) as

$$\frac{1}{H}\frac{dH}{dt} = \frac{1}{r}\frac{dr}{dt} - \frac{1}{R}\frac{dR}{dt}, \qquad \text{---} \quad \text{---} \quad \text{---} \quad \text{---} \quad \text{---} \quad (1.16)$$

Experiments show that conductivity decreases in the early
hours of the day. The specific columnar resistance r, and
hence the total columnar resistance R, also increases.
Initially, the percentage increase in r is larger than that
in R, so that H increases (see equation 1.16). Later in
the day however, when convection sets in and pollution and
water content are thoroughly mixed up in the higher levels
of the atmosphere, the percentage increase in R becomes
significant, and this is reflected in a percentage decrease
in H. The decrease in H goes on until convection reaches
its maximum in the late afternoon; after which the
percentage increase in r again dominates.

1.10. DIURNAL VARIATIONS IN THE AIR-EARTH CURRENT DENSITY

The diurnal variation of i, from equation 1.8 is given by

$$\frac{1}{I} \frac{di}{dt} = \frac{1}{V} \frac{dV}{dt} - \frac{1}{R} \frac{dR}{dt}. \quad - \quad - \quad - \quad - \quad - \quad - \quad (1.8)$$

Thus, the pattern of variation has a universal as well as a local component geared to R. Eliminating from consideration the variation in R through the use of normalized current density (see Section 1.7), we have

$$\frac{1}{I} \frac{dI}{dt} = - \frac{1}{R} \frac{dR}{dt}, \quad - \quad - \quad - \quad - \quad - \quad - \quad (1.15)$$

Hence I is determined solely by R, which in turn is determined by the total columnar nuclei content over the measuring antenna. For most stations R is maximum in the afternoon when pollution penetrates to the highest level through "austausch". Typical curves for various stations are depicted in Fig. 7. The curves of I are of course mirror images of the R-curves in the 100% - axis.
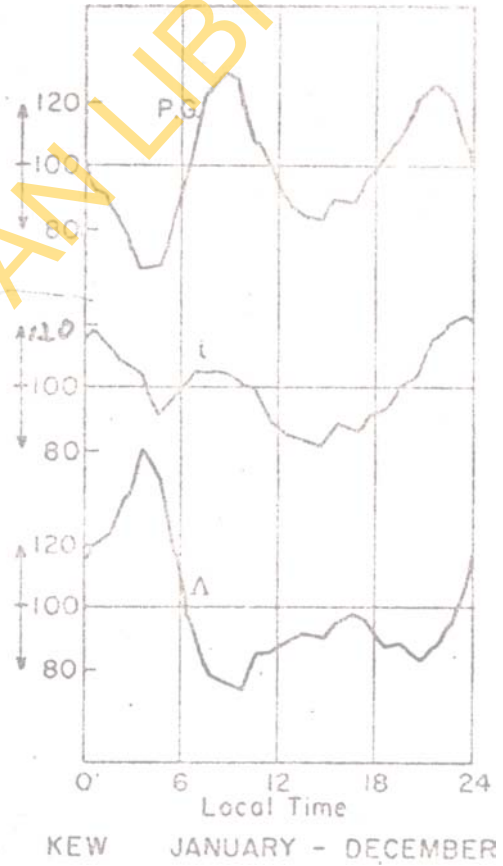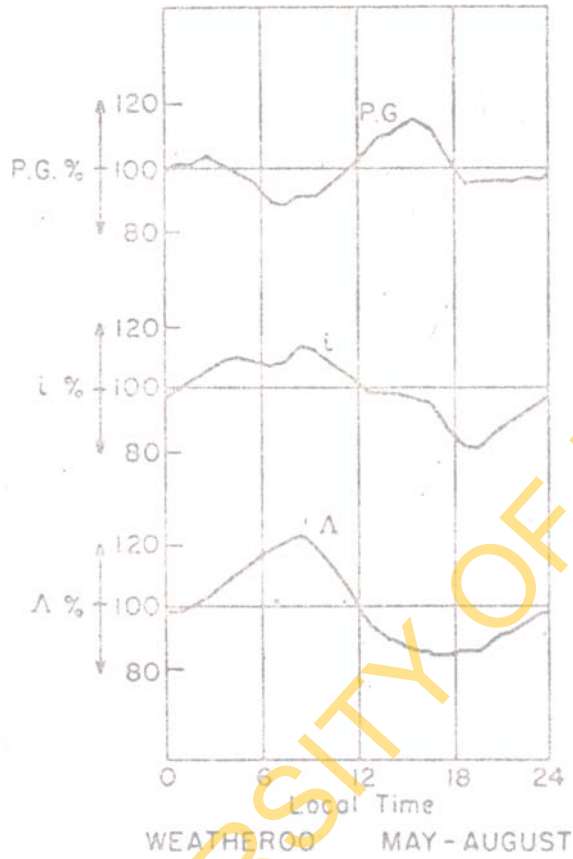
Fig 7. Atmospheric electrical state at two stations. (from Israel 1973)
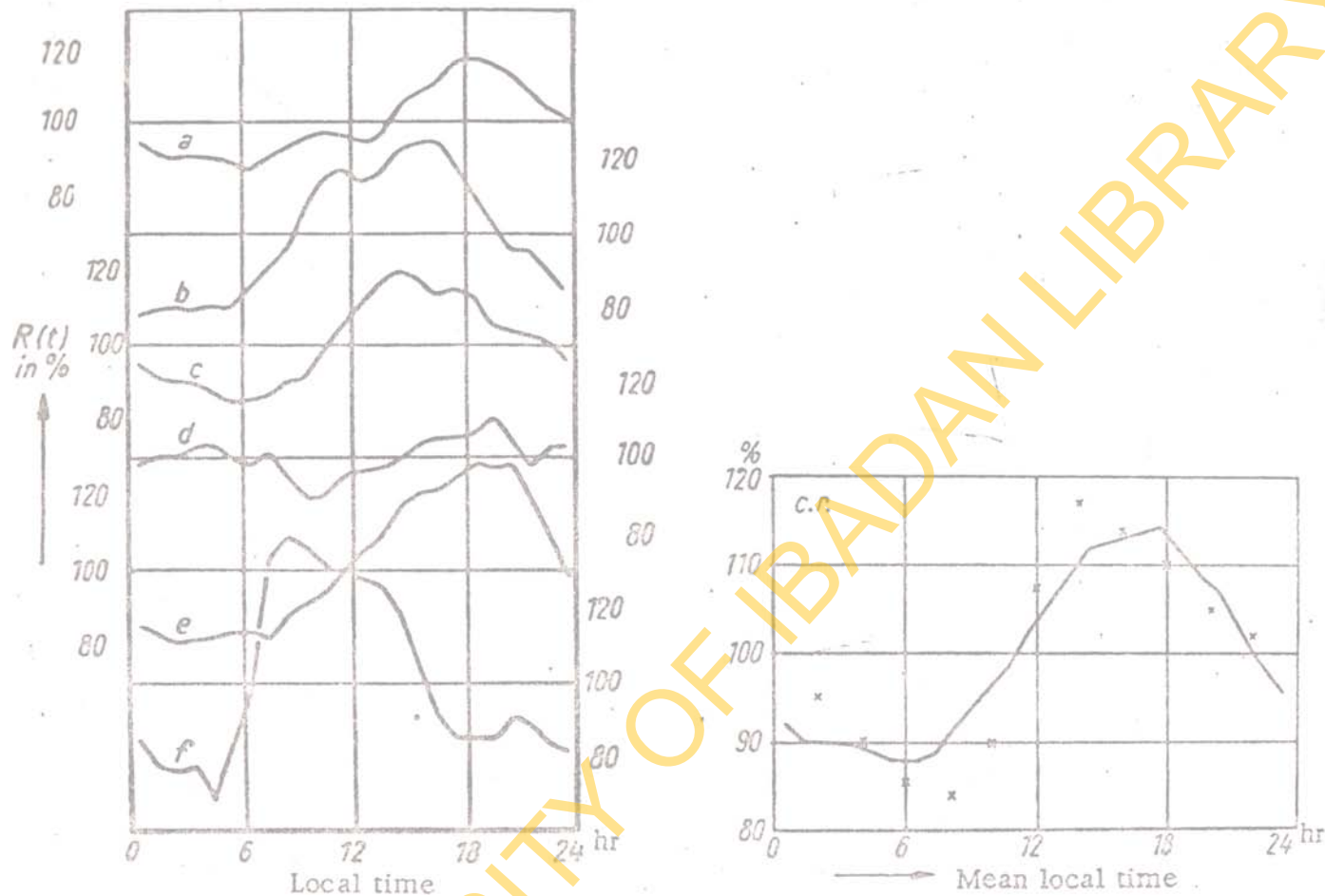
FIGURE 8. Mean diurnal variations of the c.r. $R(t)$ in %.

Left: variations at the stations: a) Spitzbergen, b) Pavlovsk, c) Potsdam, d) Wahnsdorf/Dresden, e) Kew, f) Davos. Right: Mean curve. Crosses: from conductivity measurements by R.C. Sagalyn, and co-workers   (culled from Israel 1973)

1.11. DIURNAL VARIATIONS OF CONDUCTIVITY

The diurnal variation of λ, the total conductivity of the atmosphere $(\lambda_+ + \lambda_-)$, is given by equation (1.9) as

$$\frac{1}{i}\frac{di}{dt} - \frac{1}{E}\frac{dE}{dt} = \frac{1}{\lambda}\frac{d\lambda}{dt} \qquad - \quad - \quad - \quad - \quad - \quad - (1.9)$$

Hence the diurnal pattern is controlled by local conditions, since i and E vary according to local time.

Over the oceans, the diurnal variations of potential gradient are similar to those of air-earth current and so the conductivity is virtually constant (see Fig. 4). However, for most land stations the variations of potential gradient are not single periodic as for the oceans, hence the difference in percentage variations of E and i is noticeable.

Experiments show that in the early hours of the day, conductivity increases slowly and reaches a maximum about 0800 hrs after which it decreases during 'austausch' as the small ions responsible for the conductivity become attached to large ions produced through industrial activity and traffic. The conductivity slowly recovers its night-time value as convection dies down, and the sources of pollution cease operating. The early morning increase in conductivity, like that in the air-earth current, is attributable to the sunrise effect.

1.12. HARMATTAN CLIMATOLOGY

In the period between November and March the prevailing wind in Nigeria is the E.N.E. wind. Owing to its long track over the Sahara, the E.N.E. wind is dust laden and dry. This period is locally known as the Harmattan season.

The nature of the prevailing wind results in high temperatures and low humidity during daytime, and in large diurnal temperature and humidity ranges. Visibilities are generally low in the day time particularly in the early hours of the day when condensation occurs on the dust particles. Often, low daytime visibilities cause disruption of local flight operations.

Since dust particles are charged, most electric parameters undergo pronounced depressions - often reversals - during "austausch" regime.

Ette (1973) has suggested that electrification of dust particles is due to their dispersal in the dry atmosphere.

The electrical effects associated with dust particles are closely related to dust concentrations in the atmosphere.

Analysis of the harmattan dust (Hamilton and Archibold, 1945) gave the composition: silica 50%, Alumina 10%, Lime 5%, Ferric Oxide 4%, other salts 5%. It was also observed that most of the components of harmattan dust are particles

whose diameters are very small, and that these smallest
particles are mainly responsible for producing the haze.
Here in Ibadan, Mckeown (1958) found that most of the dust
particles in the harmattan haze have diameters ranging
between 0.2 and 0.3μ.

1.13. AIM OF THE INVESTIGATION

Atmospheric electric measurements in fair-weather and
during the harmattan have been made at Ibadan by Ette
(private communication) over the period 1964 to 1968 and by
Oluwafemi (1972) over the period 1969 to 1971. In
addition to the air-earth current and the potential gradient
recorded by Ette, Oluwafemi measured the space-charge
density, as well as the windspeed near the ground. Both
workers observed reversals in the air-earth current and
potential gradient in the harmattan months during the
"austausch" regime, and attributed these to the effect of
charged dust brought down from the Sahara desert. In this
study the scope of the investigation has been further
expanded with the registration of three additional relevant
parameters - the dust concentration and the polar
conductivities.

The amount of data obtained has unfortunately been
limited by the fact that the dust monitor, used for the

registration of dust concentration in the air was only
functional between December 1978 and February 1979, during
which period the field mill for the potential gradient
measurements was not operational, and some data for the
air-earth current were missed. Taken in conjunction with
data kept for the station for the period 1964-1971 however,
the available data do provide useful information about the
atmospheric electric climate at Ibadan during the harmattan
season.

1.14.   EXPERIMENTAL SITE

Recordings were carried out in two huts at the
departmental experimental site at Ibadan (lat. 7° 24'N,
long. 3° 54'E). The layout at the site is shown in Fig. 9.
Hut I in the figure housed the amplifiers for conductivity,
space-charge and air-earth current measurements; while hut
2 accomodated the dust monitor assembly and recorders for
continuous registrations of the dust concentration, wind
speed and wind direction. The anemometer for sensing the
wind parameters, was positioned at point B in the figure at
a height of about 10m above the ground; while the air
intake for the dust monitor was through a chimney stack at
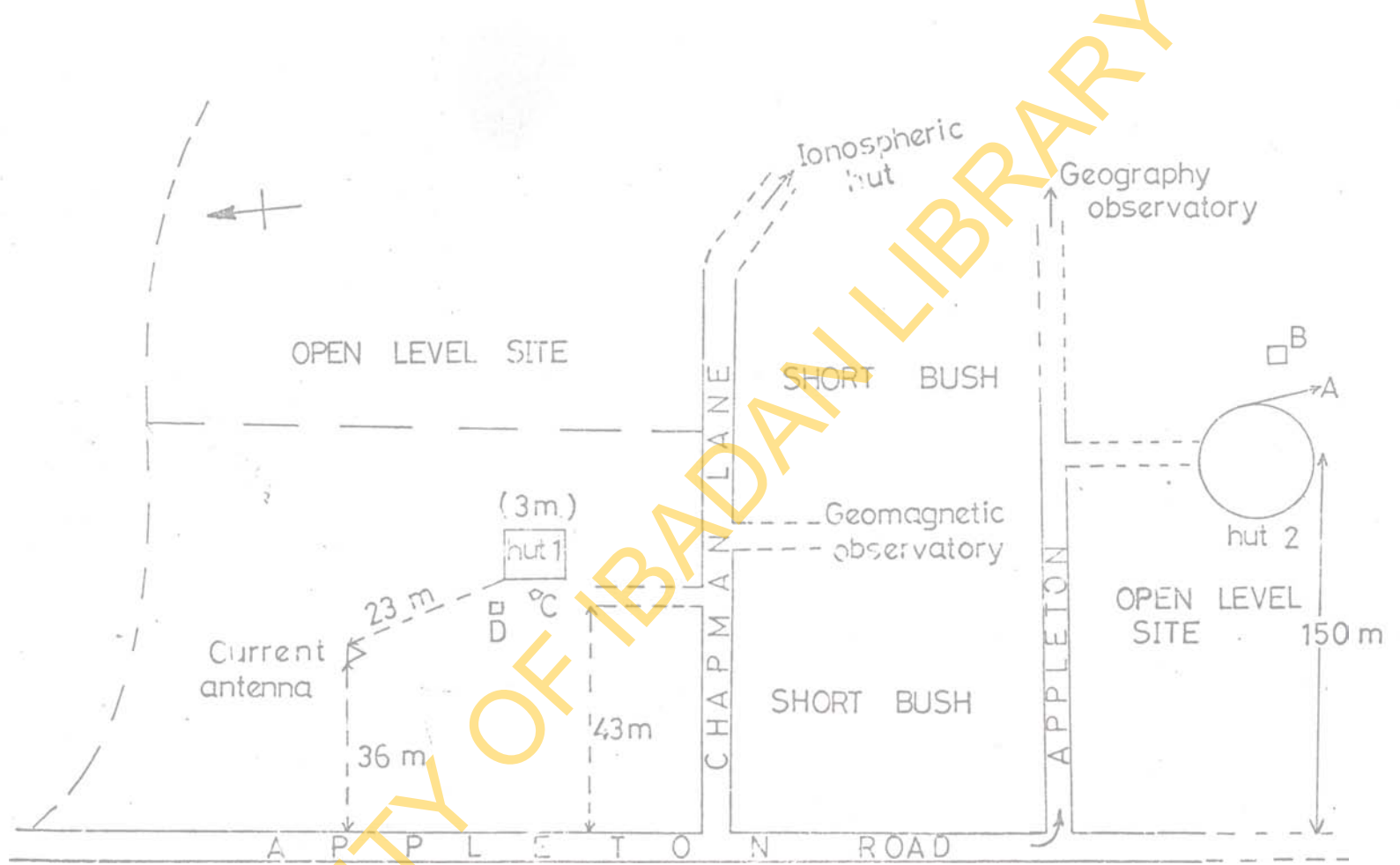
Fig. 9   Plan of   Experimental   Site.

A = Air   intake   for   dust   sampler   (2·5m)
B = Mast   carrying   anemometer (10 m)
C = Space   charge   filter   (0·5m)
D = Conductivity   meters   (1 m)

a height of about 2.5 meters above the ground. The loca-
tions of other sensors used in the investigations are as
indicated on the diagram.

2.1. AIR-EARTH CURRENT MEASUREMENT

The arrangement for measuring the air-earth current has already been described in detail by Ette (1966) and Oluwafemi (1971) and is illustrated schematically in Fig. 10). The current antenna, a **tri**angular stainless steel wire mesh (see Fig. 10a) was mounted on three all-weather insulators designed by Ette (1966).

2.1.1. Measurement Principle

The schematic arrangement for measurement is depicted in Fig. 10. Charges collected by the antenna A leak to earth through the resistor R whose value could be changed by a range switch; and the resulting current was measured by a Keithley model 301 operational amplifier connected up in the differential current mode.

To balance out spurious signals generated in the long signal cable, due for instance to temperature or pressure changes, an identical dummy cable fed differentially into the amplifier as shown.

Thus if V_o is the output voltage from the amplifier,

Fig. 10   Air-earth   Current   Antenna.

(a)
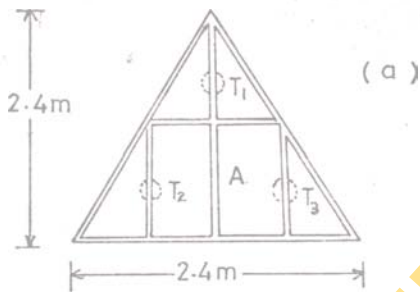
A = Triangular stainless
    steel wire mesh
    antenna.

T_1, T_2, T_3 = All-weather
    insulators

B_1 = Screened signal
    cable.

B_2 = Screened dummy
    cable.

R = $10^{10} - 10^{12} \, \Omega$ (switched)

C = 4700 pF

(b)
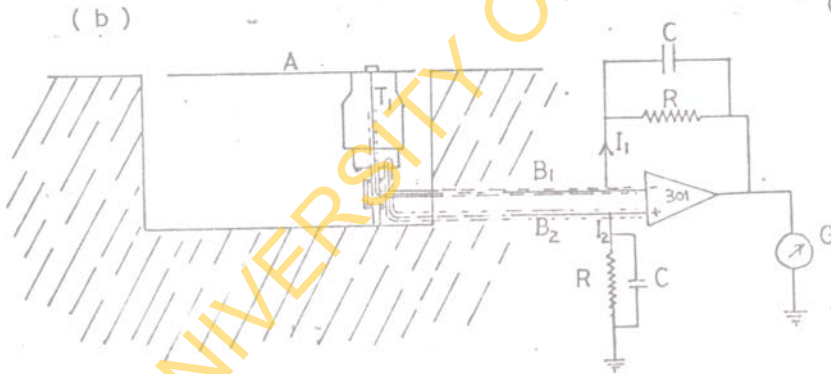
we have

$$V_o = R(I_2 - I_1)$$

Convection currents, likely to be significant during harmattan conditions when there are large concentrations of moving charged dust, were suppressed by the use of a wire-mesh antenna. Since the effective area of the antenna for convection currents is the sum of the projections of the areas of the individual wires on the horizontal plane, while the effective area for conduction current is the area of the triangular outline of the antenna, it is clear that the antenna responds essentially to conduction and displacement currents only.

A Kasemir (1955) matching network, consisting of a parallel combination of R and C (with RC $= \varepsilon_0/\lambda$, the relaxation time of the atmosphere at ground level), effectively filtered out the displacement current component, leaving only the conduction current.

In the investigation, RC was fixed at 470s.
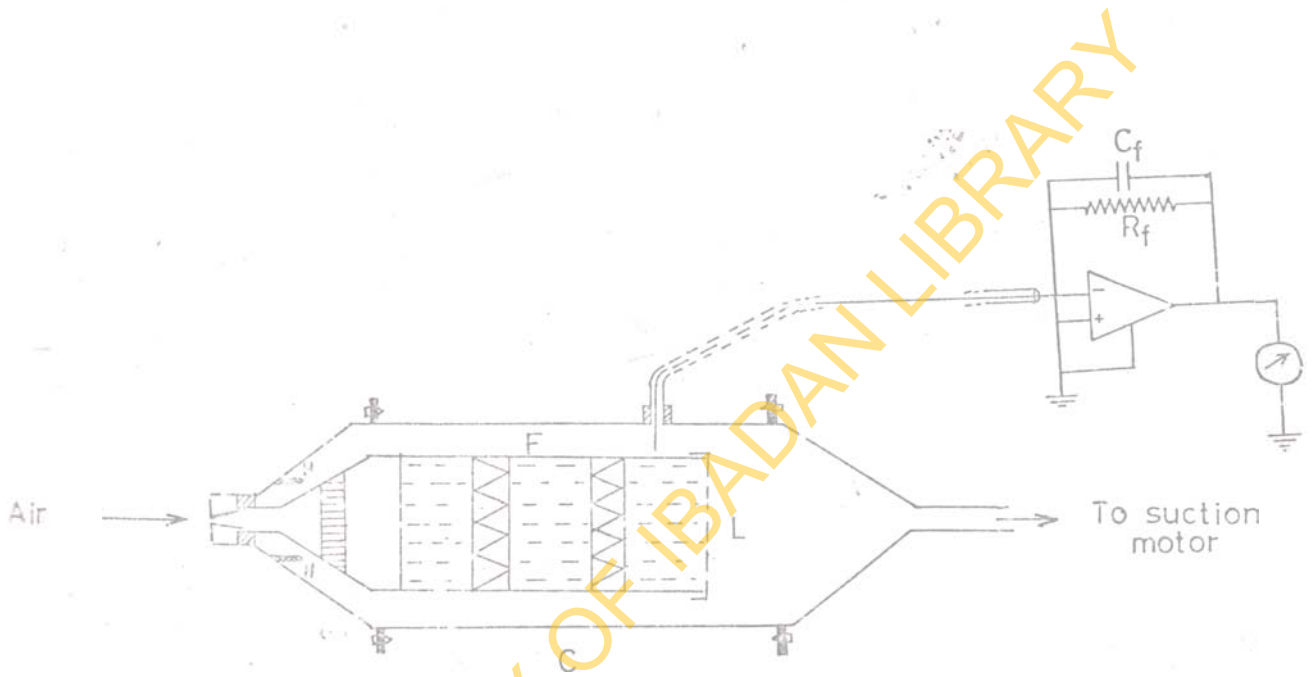
Fig 11   The space charge collector

H = Heaters
C = Metal case
F = Filter catridge
L = Removable perforated lid

▨ Teflon insulation
☰ Steel wool
⊞ Glass wool fibres
▷ 'Drager' filters
▦ Rubber seals

2.2.   SPACE-CHARGE MEASUREMENTS

The space charge density near the ground was measured by means of a space-charge filter of the Bent (1964) construction; the insulating support for the filter assembly being modified as already described by Oluwafemi (1971). Two Drager S.T. filter papers formed the basic filter elements for trapping charges in the air. These were mounted inside the metal filter cartridge F between steel wool and glass wool filters; and the charges collected as air was sucked at a constant speed through the filter were measured using a Keithley model 301 operational amplifier connected up in the linear current mode as shown in the diagram (Fig. 11). The suction rate was measured on an anemometer built into the suction motor.

To prevent condensation of moisture on the filter insulator at night a heater H was installed near it to keep it warm.

2.2.1.   Operational Principles

Air is sucked through the space charge filter at an average rate of L linear feet per minute, say. With the inlet area of A sq. feet, the flow rate of the sampler is given as

$$Q = LA \text{ (cu.ft/min)} \quad - \; - \; - \; - \; - \; - \; - \quad (2.1.)$$

Now, 1 cu.ft/min $= 2.7 \times 10^4 (cm^3/min) = 450 \; cm^3 s^{-1}$

$$\therefore Q = 450LA \; cm^3 s^{-1} \quad - \; - \; - \; - \; - \; - \quad (2.2)$$

i.e. 1 linear feet/min $= 450A \; (cm^3 s^{-1})$

In the arrangement used inlet diameter was 7/8"; and so

$A = 4.156 \times 10^{-3} sq.ft.$

Hence $Q = 1.88L \; cm^3 s^{-1}$; and the space charge density ρ is

obtained as

$$\rho = \frac{I_a}{Q} \times 10^{-6} Cm^{-3}$$

$$= \frac{I_a}{1.88L} \times 10^{-6} Cm^{-3} \quad - \; - \; - \; - \; - \; - \quad (2.3)$$

I_a(in Amp) being the net space charge current as measured by
the operational amplifier.

2.3. CONDUCTIVITY MEASUREMENTS

The positive and negative conductivities were measured
by means of Gerdien capacitors through which air was drawn
by means of suction motors. The capacitors, each consisting
essentially of an insulated brass rod mounted coaxially
inside a large hollow brass cylinder, were arranged side by
side on a wooden stand at a height of about 1m, as shown in

Fig. 13.

Details of the construction of each tube are shown in
Fig. 12 .

2.3.1. Operational Principles

With air drawn slowly through a Gerdien tube, between
whose electrodes a fixed potential difference V_{in} is applied,
a leakage current, which is a measure of the conductivity,
flows between the electrodes. This current I_{in}, which is
very small is measured using an electrometer as the potential
difference across a high resistance R between the cylinders.
The schematic arrangement used for measuring the positive
polar conductivity is shown in Fig. 12.

A similar arrangement, but with the applied potential
difference reversed, was used to measure the negative polar
conductivity.

2.3.2. Theory

The output voltage V_o from the electrometer is given by

$$V_o = - I_{in} R_f \qquad \qquad \qquad - - (2.4)$$

$$= - \frac{Q}{\varepsilon_o} \lambda R_f \qquad \qquad \qquad - (2.5)$$

where ε_o/λ, the time constant of the air, represents the
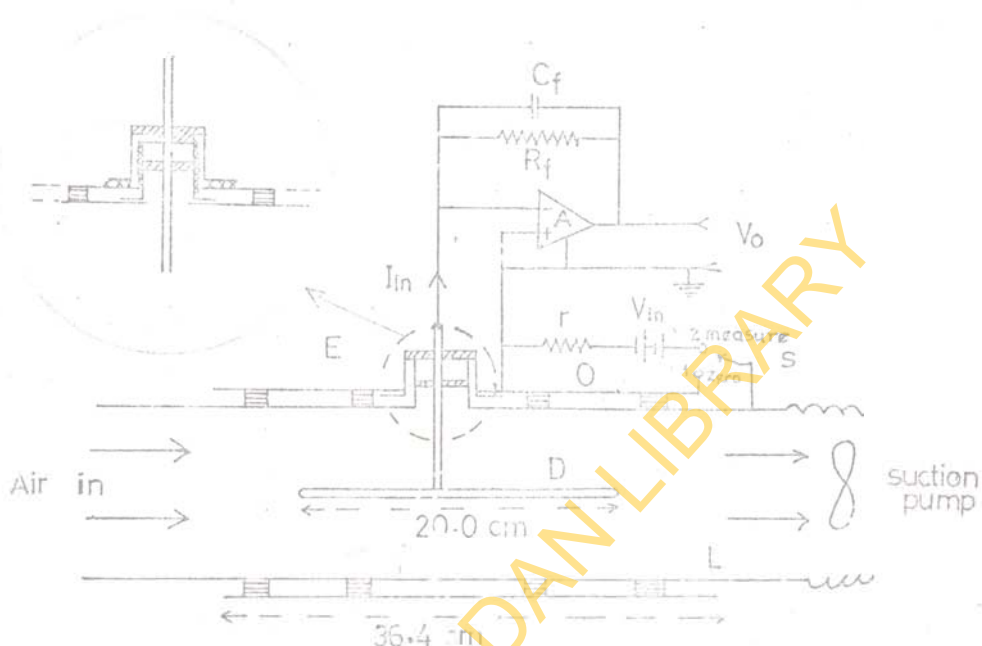
Fig 12   Electrical connections in the meter
for measuring positive conductivity.

C_f = Feedback capacitor = 270 pF

R = Feedback resistor = 10^{12} Ω

A = Keithley model 301 operational
amplifier

r = 10^6 Ω

V = 47·5 volts

S = In-built double pole switch

O , D, L = Brass cylinders

⊟ Tufnol   ▨ Teflon   ▯ Heating coil   ▭ Rubber seal

Fig 13: The conductivity meters

rate at which the central electrode loses charge.

Since $Q = C.V_{in}$ — — — — — — — — (2.6)

we have $\lambda = \dfrac{\varepsilon_o V_o}{CV_{in}R_f}$

for each of the Gerdien tubes,

$C = 5.88 \times 10^{-12}$ F

$R_f = 10^{12}$ Ω

$V_{in} = 47.5V$, supplied by a dry cell.

Hence $\lambda = 3.168 \times 10^{-14} V_o$ (Ω^{-1}m^{-1}) — — — (2.7)

In order to eliminate oscillations of the electrometer amplifier output and minimise the effect of displacement currents resulting from sudden changes in the potential of the central electrode when the applied potential difference V_{in} is switched on or off, a capacitance of 270pF was connected across R_f.

2.4.   MEASUREMENT OF DUST CONCENTRATION

2.4.1.   General Remarks

There are two methods of measuring the concentration of dust in the atmosphere, the direct (weigh ing) and the indirect methods. The direct gravimetric techniques are not easily available for automatic and continuous operation.

Indirect methods involve measuring a parameter or a **property** of the particle which can be related to its mass. These methods are based on light scattering, light transmission, α-, β- or γ-radiation attenuation. β-radiation attenuation method was chosen in this work because β-radiation is a function of the mass of the absorbing matter, while the other properties of the absorbing matter are not affected by the attenuation process.

2.4.2. Measuring Principle

The beta absorption principle, which is independent of the physical, chemical and optical properties of the dust, is employed for highest accuracy in measuring the concentration of dust in the atmosphere.

The instrument used is the Phillip's dust monitor model PW9790 and the measurement scheme is illustrated in Fig. (14). Radiation from a beta source is allowed to pass through a portion of a clean glass-fibre filter tape and the radioactivity of the tape counted by a Geiger-Muller counter. **Over a preset counting period**, the output pulses from the counter are counted by an electric up-down counter.

The same portion of the filter tape is then exposed to dust and once again exposed to the beta radiation. The output pulses of the detector are then used to count down to zero from the number obtained using the clean tape. More of
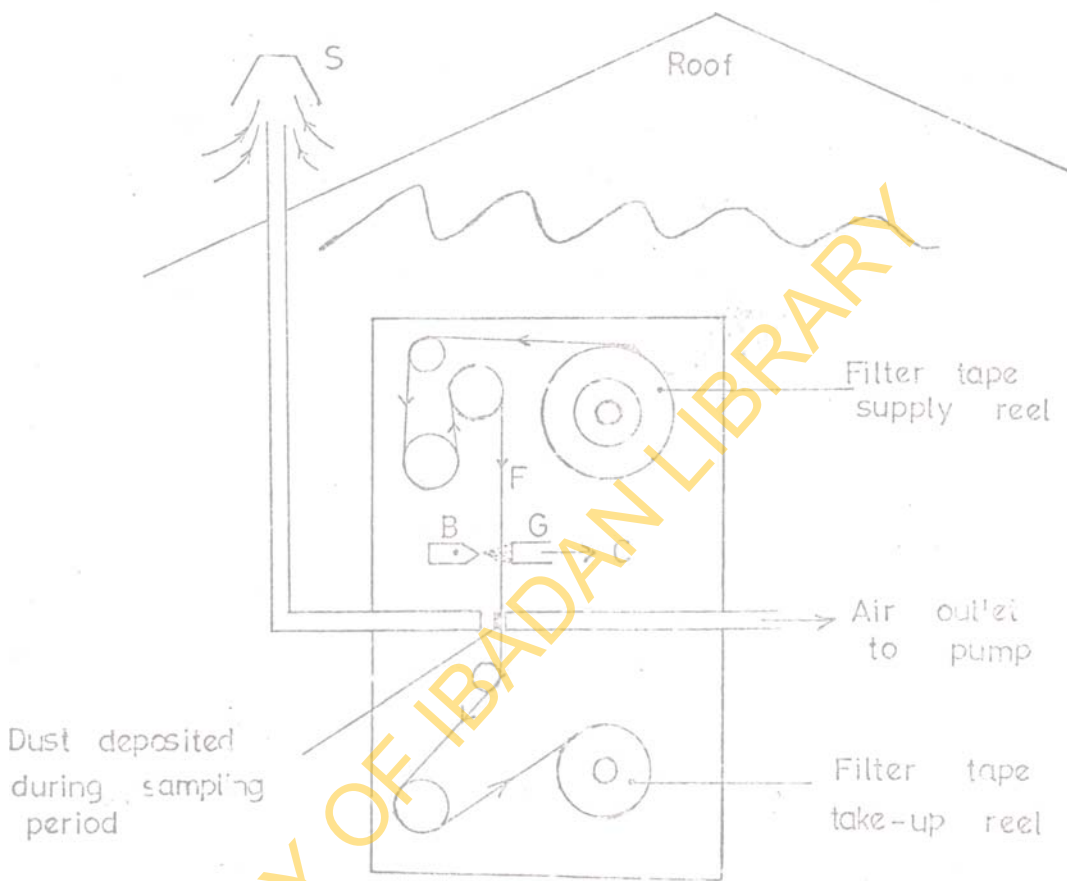
Fig. (14) Diagramatic representation of the
measurement unit.

S = dust sampler to restrict size
of dust
F = Filter tape
B = Beta source
G = Geiger - Müller detector
C = Up - down counter

the radiation is absorbed because of the dust layer on the filter tape, resulting in a lower count-rate.

The time taken to count down to zero is therefore longer than the preset counting period. The difference in time between the up-counting and down-counting periods is a measure of the mass of dust on the filter.

2.4.3. Symbols Used

I_o - Intensity of β-radiation at source

I - Intensity of β-radiation at detector

K - mass absorption coefficient for source/ detector pair

N - Count rate of detector (G.M. Tube)

N' - Count rate of detector for clean tape.

T_s - Couting period for clean tape.

N_T - Total count reached over time T_s at count rate N'

$$N_T = N'T_s$$

N'' - Count rate of detector for dust-laden tape ($N'' \angle N'$)

$\triangle t$ - Additional counting period for count N_T to be reached with dust layer on tape; $N_T = N'' (T_s + \triangle t)$

T_{AC} - Sampling period (time taken to accumulate dust on tape).

A - Surface area of dust layer on tape.

Q - Pump flow-rate

C - Ambient concentration of dust in the atmosphere.

m - Mass per unit area of dust layer.

$\triangle m_o$ - Mass per unit area of clean tape.

$\triangle m_T$ - Total mass per unit area.

V - Amplitude of pulse.

2.4.4. Theory of Method

Attenuation of the β-radiation is an exponential process represented by the equation (From Manufacturers manual)

$$I = I_o e^{-K.\triangle m_T} \quad - - - - - - - - - \quad (2.8)$$

The count-rate of detector is proportional to the intensity of β-radiation, i.e. $N = \alpha I$, α is a constant

$$\therefore N = \alpha I_o e^{-K.\triangle m_T} \quad - - - - - - - \quad (2.9)$$

The count-rate N' measured through the clean tape is given as

$$N' = \alpha I_o e^{-K.\triangle m_o}$$

During the counting period T_s, the total count N_T is given as $N_T = N'T_s$

$$\text{or } N_T = \alpha I_o T_s e^{-K.\triangle m_o} \quad - - - - - - \quad (2.10)$$

With a layer of dust on tape, count rate N" obtained is given as

$$N" = \alpha I_o e^{-K(\triangle m_o + \triangle m)} \quad - \ - \ - \ - \ - \ - \ - \ - \ (2.11)$$

To obtain the same total count N_T at N" count-rate, a longer period of time, $T_s + \triangle t$ is required.

$$\therefore N_T = N" (T_s + \triangle t)$$

$$\text{or } N_T = \alpha I_o (T_s + \triangle t) e^{-K \cdot (\triangle m_o + \triangle m)} \quad - \ - \ - \ (2.12)$$

From equations (2.10) and (2.12) we have

$$T_s \alpha I_o e^{-K \cdot \triangle m_o} = \alpha I_o (T_s + \triangle t) e^{-K(\triangle m_o + \triangle m)}$$

Hence $\quad \dfrac{T_s + \triangle t}{T_s} = \dfrac{e^{-K \cdot \triangle m_o}}{e^{-K(\triangle m_o + \triangle m)}} = e^{k \triangle m}$

Taking logarithms of both sides gives

$$\log_e (1 + \frac{\triangle t}{T_s}) = K \cdot \triangle m \quad - \ - \ - \ - \ - \ - \ (2.13)$$

$$\therefore \quad \triangle m = \frac{1}{K} \log_e (1 + \frac{\triangle t}{T_s})$$

The total amount of dust collected on the tape is $\triangle m.A = C.Q.T_{AC}$; whence $C = \dfrac{\triangle m.A}{QT_{AC}}$,

$$\text{or} \quad C = \frac{A}{QT_{AC}K} \cdot \log_e (1 + \frac{\triangle t}{T_s}) \quad - \ - \ - \ - \ - \ - \ (2.14)$$

This equation can be used to compute the dust concentration

accurately.

On expansion, the logarithmic term gives

$$\log_e(1 + \frac{\triangle t}{T_s}) = \frac{\triangle t}{T_s} - \frac{1}{2}(\frac{\triangle t}{T_s})^2 + \frac{1}{3}(\frac{\triangle t}{T_s})^3 + \ldots + \ldots$$

Assuming $\triangle t \ll T_s$, which is the case in practice, then first order approximation could be used.

$$\therefore \log_e(1 + \frac{\triangle t}{T_s}) = \frac{\triangle t}{T_s}$$

putting this in equation (2.14) gives

$$C = \frac{A.}{K.T_s.Q.T_{AC}} \triangle t \qquad \qquad (2.15)$$

The digital-to-analog converter on the output circuit board which is situated in the control unit gives an analog voltage V which increases linearly with $\triangle t$, so

$$V = B.\triangle t \qquad \qquad \qquad (2.16)$$

where B is a known constant.

$$\therefore \triangle t = \frac{V}{B} \text{ and equation (2.15) becomes}$$

$$C = \frac{A.V}{B.K.Q.T_s.T_{AC}} \qquad \qquad (2.17)$$

for calibration, $V = 5.5$ volts, $T_s = 2$ mins and $A = 2cm^2$ when a standard foil with $\triangle m = 0.75mg/cm^2$ is used. Hence from equation (2.17) we have

$$V = B.K. \frac{C}{A}.Q.T_{AC}.T_s \quad — \quad — \quad — \quad — \quad — \quad — \quad (2.18)$$

$$V = B.K \triangle m \, T_s, \quad — \quad — \quad — \quad — \quad — \quad (2.19)$$

where

$$\triangle m = \frac{C \, Q \, T_{AC}}{A}$$

Using equation 2.19, we have

$$5.5 = B.K \times 0.75 \times \frac{2}{60}$$

or $B.K. = \dfrac{5.5 \times 60}{0.75 \times 2}$

$$= 220$$

Hence with $A = 2cm^2$, equation 2.18 becomes

$$V = 220 \times \frac{1}{2} \times C.Q \times T_{AC} \cdot \frac{2}{60}$$

$$= \frac{11}{3}.C.Q.T_{AC}$$

whence $C = \dfrac{3}{11.0} \cdot \dfrac{V}{Q \cdot T_{AC}} \quad — \quad — \quad — \quad — \quad — \quad (2.20)$

In the set-up used, $T_{AC} = 50$ min and $Q = 1.1 m^3/hr$, so that $C = \dfrac{3}{11} \cdot \dfrac{1}{1.1} \cdot \dfrac{60}{50} \cdot V = \dfrac{3}{11} \times \dfrac{6}{5.5} V$

$$= 0.277V \ (mg/m^3)$$

$$\therefore \bar{c} = 280 \pm 40 \, V \, \left(\mu g \middle| m^3\right) \qquad - \quad - \quad - \qquad (2.21)$$

This was the final formula used in determinations of dust concentration from the chart recordings.

2.5. AMPLIFIERS

In most of the measurements made, a Keithley model 301 operational amplifier was used to amplify the very small input signals. The amplifier can be connected up in several modes to suit the particular measurement contemplated.

For the air-earth current measurements, the amplifier was connected up in the differential linear current mode, as illustrated in Fig. 15a; while for conductivity and space-charge density measurements the amplifier was connected up in the linear current mode illustrated in Fig. 15b.

The specifications of the model 301 amplifier are given in the appendix. The amplifiers for the measurements were powered by Keithley model 3012 power supplies giving voltages of ±25v.
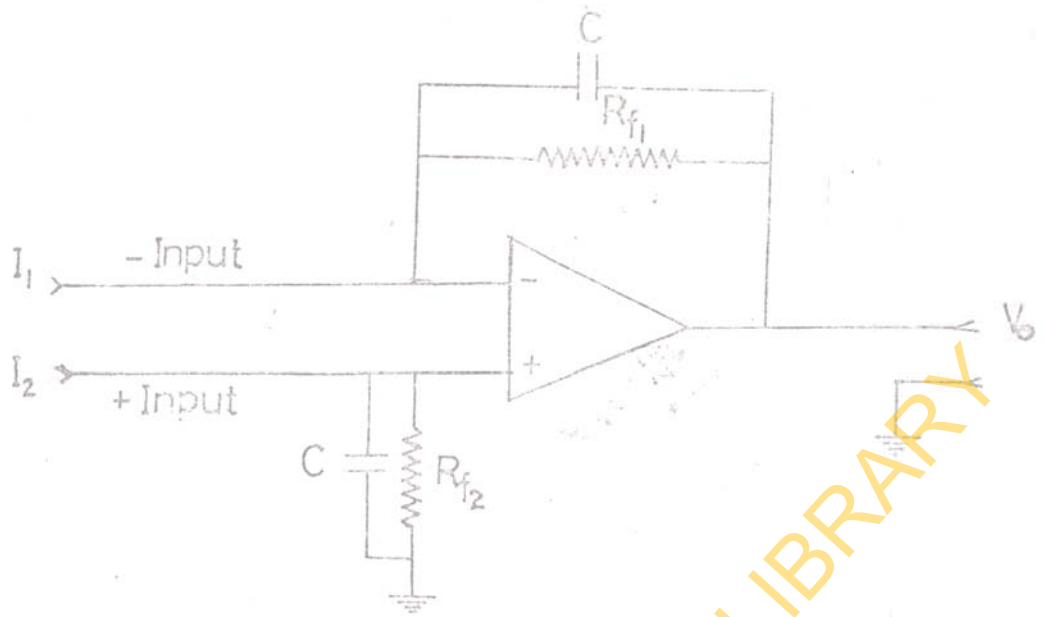
Fig 15a   Differential   Linear   Current   Amplifier
                  Without   Fractional   Feedback.

$$R_{f_1} = R_{f_2} = 10^{10} \ \Omega$$

$$V_0 = R_f (I_2 - I_1)$$

$$V_0 = 10^{10} (I_2 - I_1), \text{ Volt}$$

where I_1 =   Input   from   the   signal   cable

I_2 =   Input   from   the   dummy   cable

C =   4700   pF
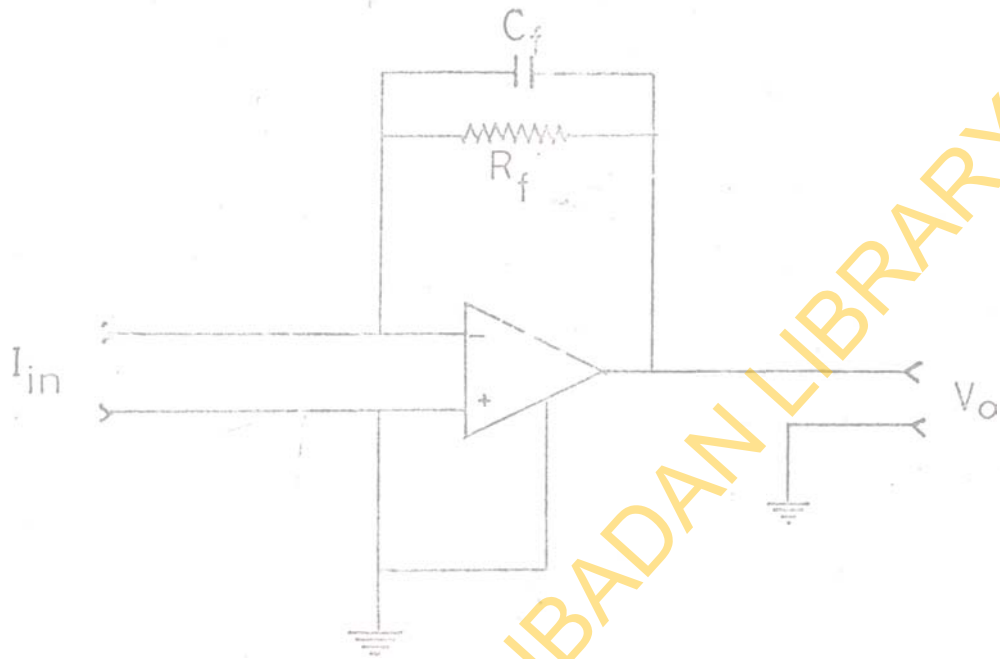
Fig. 15b Linear   Current   Amplifier
          Without   Fraction Feedback

$R_f = 10^{11} \ \Omega$

$C_f = 270 \ pF$

$V_o = -I_{in}R_f$

2.6. RECORDERS

Four different types of recorders were employed in the systematic recordings of the various elements studied. These include

(1) The Record signal amplified Galvanometric triplex recorder, used for recording the polar conductivities,

(2) the Record duplex graphic recorder used for the air-earth current density and the space charge density recordings

(3) the Philips' model PM8202 single-line recorder used for recording the dust concentration and

(4) the Philips' PCS-Recorder used for continuous recording of the wind speed and wind direction simultaneously.

Recorders specified in (1) and (2) were installed in experimental hut I while those in (3) and (4) formed part of the Philips PW9790 dust monitor and PW9737 anemometer installed in hut 2 (Fig. 9).

The duplex and triplex recorders used have basically the same electrical characteristics; each channel having an internal resistance of $1.1K\,\Omega$ and being capable of measuring currents in the range $-125\mu A-0-125\mu A$. ($-100\mu A-0-100\mu A$ in the case of the triplex). Synchronous electric motors with dual speed chart drive provide a choice of two chart speeds — 1 inch and 6 inches per hour.

The measuring system of the PM 8202 recorder, supplied with the dust monitor, is a potentiometric auto-balancing D.C. amplifier having very low zero-point drift and an input resistance of 1M Ω.

The chart drive is a digitally controlled stepper motor giving chart speeds of 20-640mm/hr and 20-320mm/hr.

The PCS-recorder is an electrically driven recorder with a fixed chart speed of 30mm/hr; and since both the wind speed and direction are recorded on a single chart the pens for them are arranged to have different colours.

CHAPTER III

3. RESULTS

3.1. Presentation of Data

Measurements were made, during the harmattan months (November 1978 to March 1979) of the electric elements - space charge density, polar conductivities, air-earth current - as well as the meteorological elements - dust concentration and wind speed. Records of temperature and relative humidity obtained routinely at the Geography observatory in the University provided additional meteorolo- gical parameters from which the vapour pressure was deduced. The vapour pressure was calculated as relative humidity expressed as a fraction, multiplied by the saturation vapour pressure of water at the relevant temperature. Values of saturation vapour pressure at different temperatures are given in Table 2.

Values of each parameter averaged over hourly intervals, were obtained from the records, and the monthly mean of each hourly value expressed as a percentage of the total monthly mean of the parameter.

The absence of potential gradient values notwithstanding,

diurnal variations in that.parameter could be studied from

the equivalent parameter H, obtained as

$$\frac{1}{H}\frac{dH}{dt} = -\frac{1}{\lambda}\frac{d\lambda}{dt} - \frac{1}{R}\frac{dR}{dt} \; ; \; \text{or}$$

$$\frac{1}{H}\frac{dH}{dt} = \frac{1}{I}\frac{dI}{dt} - \frac{1}{\lambda}\frac{d\lambda}{dt} \; - \; - \; - \; - \; - \; - \; - \; (3.1)$$

3.1.1. Diurnal Variations of the atmospheric Electric

and Meteorological Elements: The mean diurnal variations

or the atmospheric electric elements are presented in Figs.

16 for the three months (January to March 1979) for which

air-earth current records are available. The meteorological

elements for the same harmattan period are shown in figs 17.

For comparison, the diurnal curves.of H and I for this station,

with H computed as $E_{station}/E_{ocean}$, are given in Figs. 18 for

the harmattan months of 1964, 1965, 1968 and 1969 using data

obtained by Ette (private communication). It should be noted

however that since ths data were analysed with.a view to studying

the fair-weather atmospheric electric slimate, records for

pronounced harmattan conditions were not included in the analysis.

This selective data analysis is possibly responsible for the lack of

simflitude of some of the resulting diurnal curves with those obtained
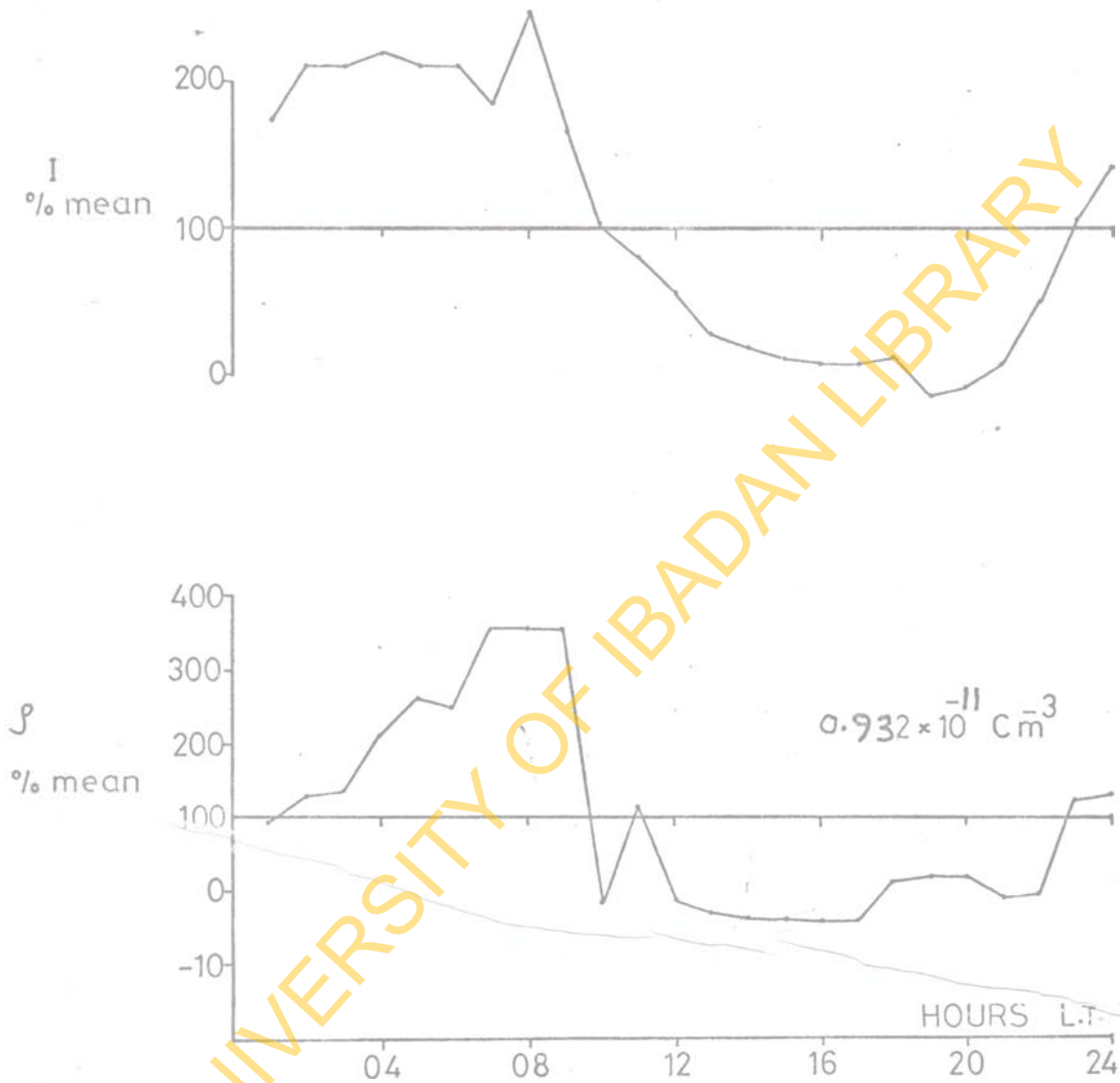
Fig.16a. Diurnal variations of I and ρ for January 1979.
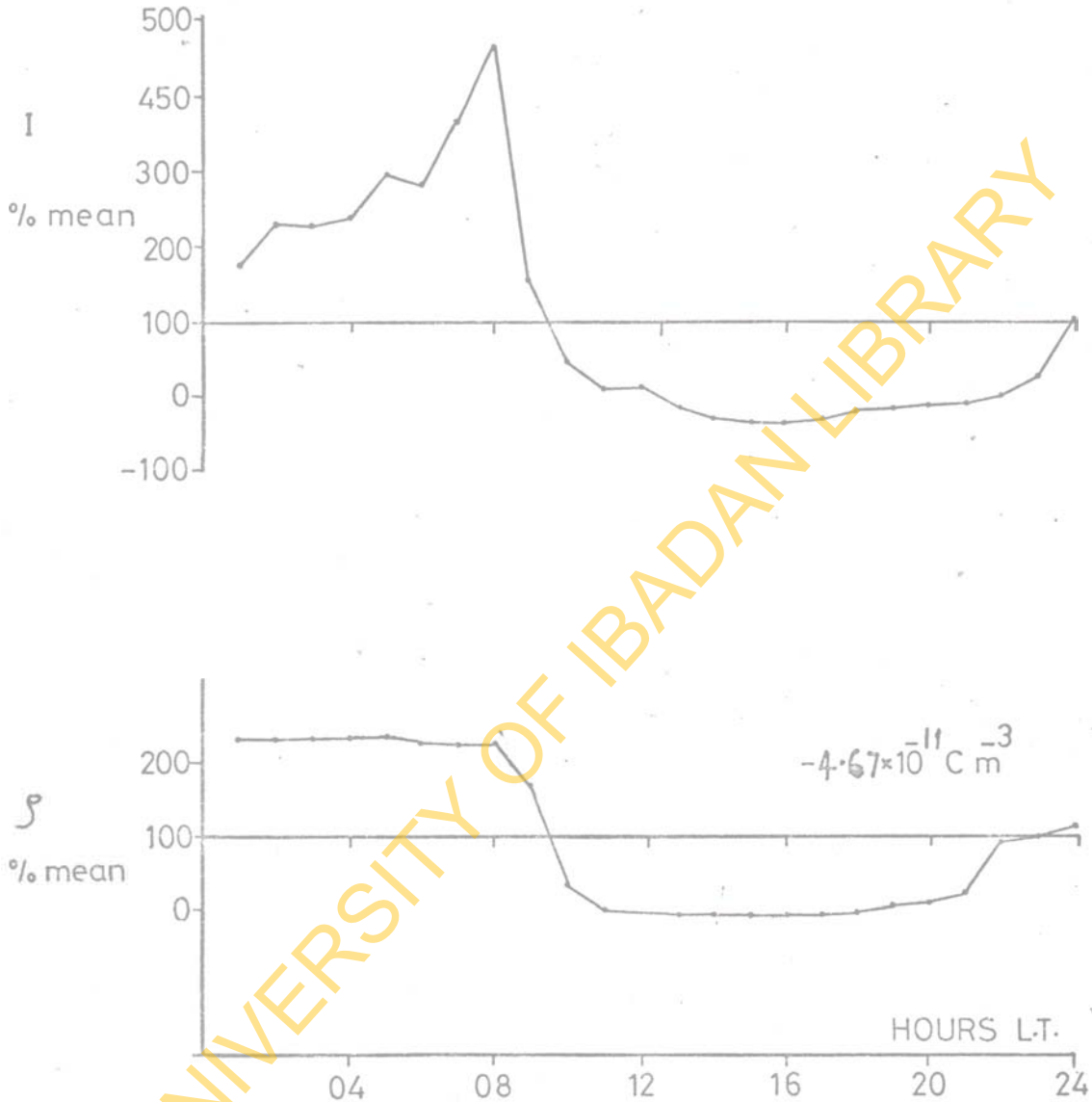
Fig. 16b. Diurnal variations of I and $\mathcal{S}$ for
February 1979.
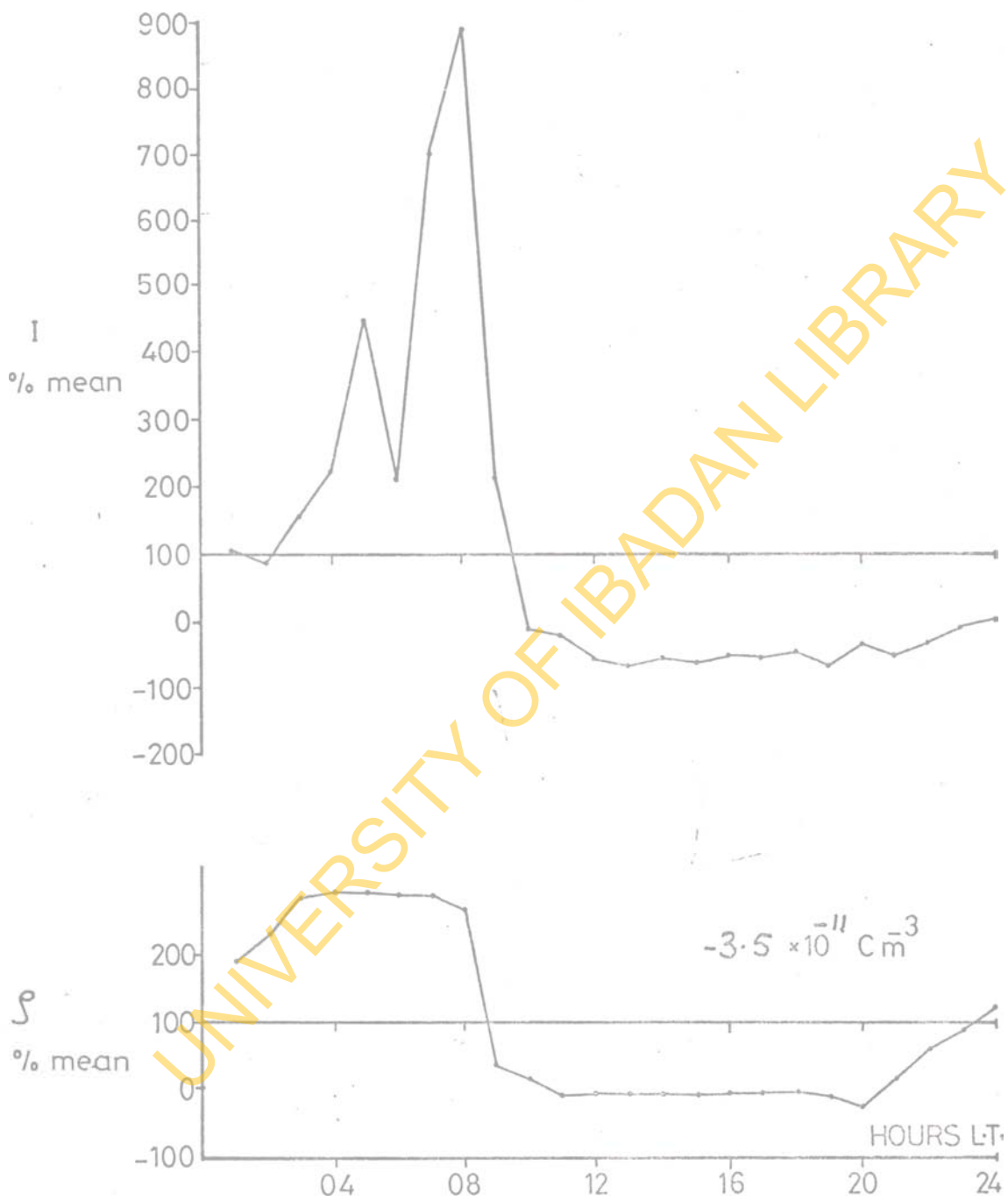
Fig.16c.   Diurnal   variations   of   I   and $\mathcal{S}$
for   March   1979.
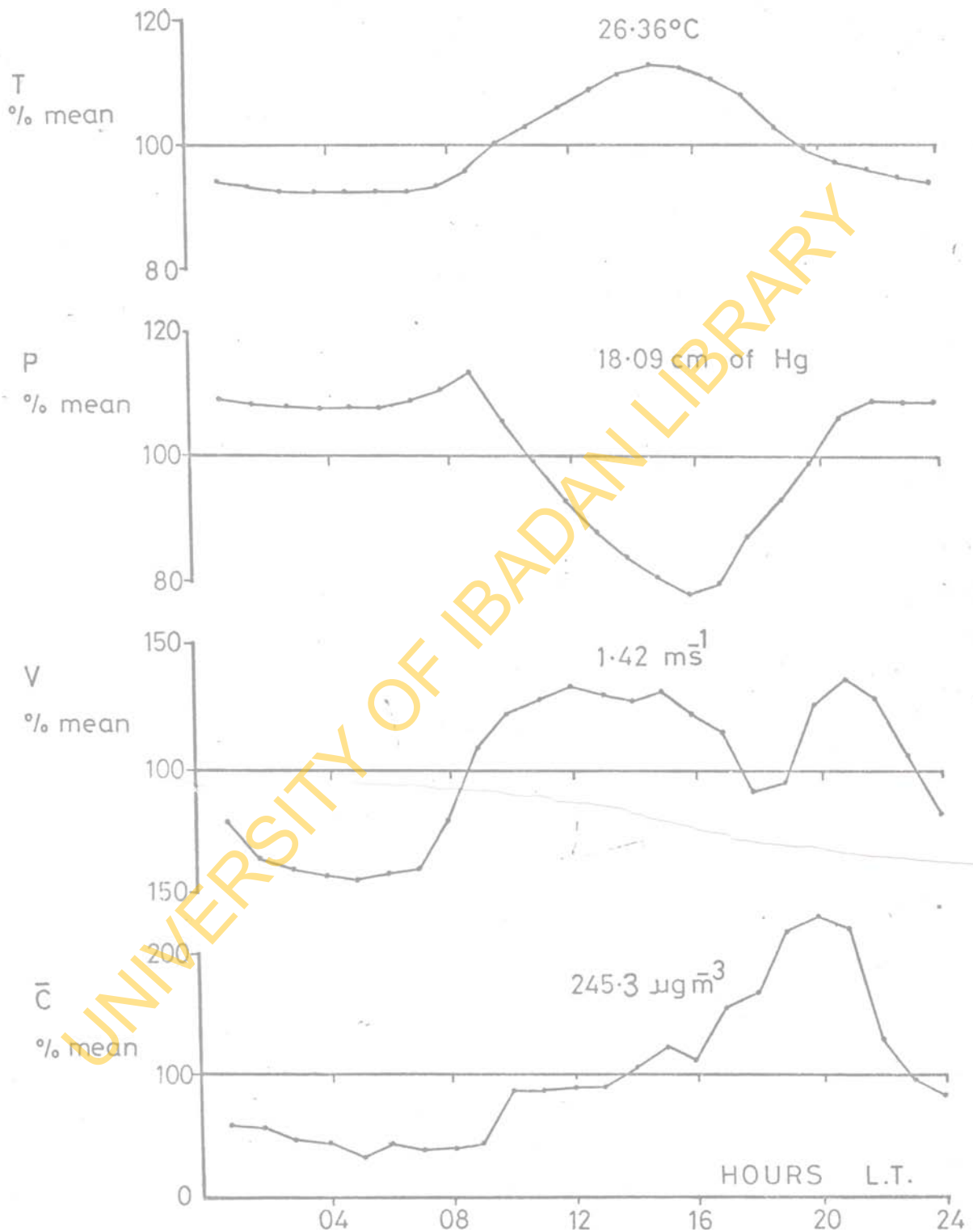
Fig.17a. Diurnal variations of T, P, V and $\bar{C}$ for December 1978.
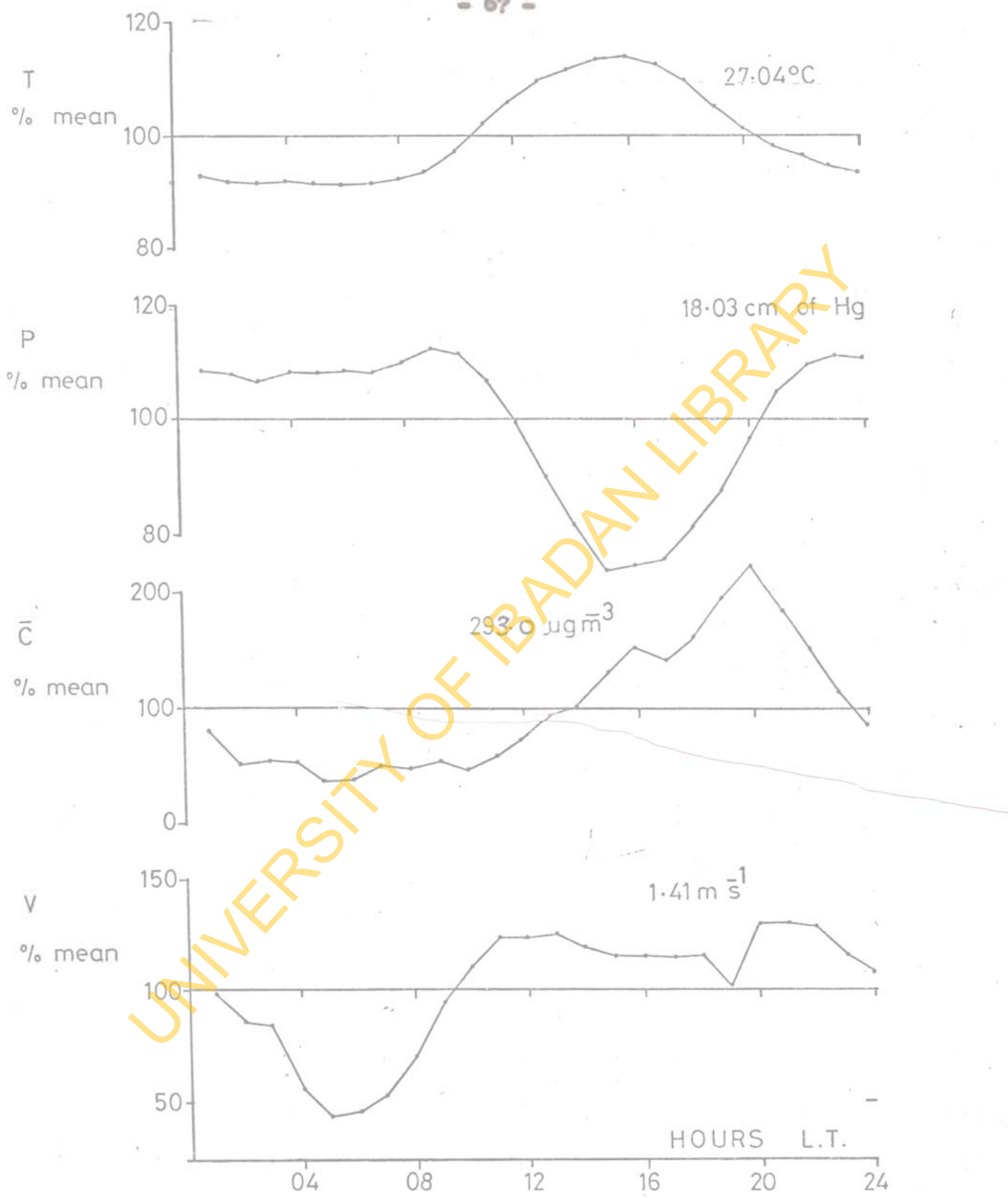
Fig.17b. Diurnal variation of the meteorological elements T, P, C̄ and V for January 1979.
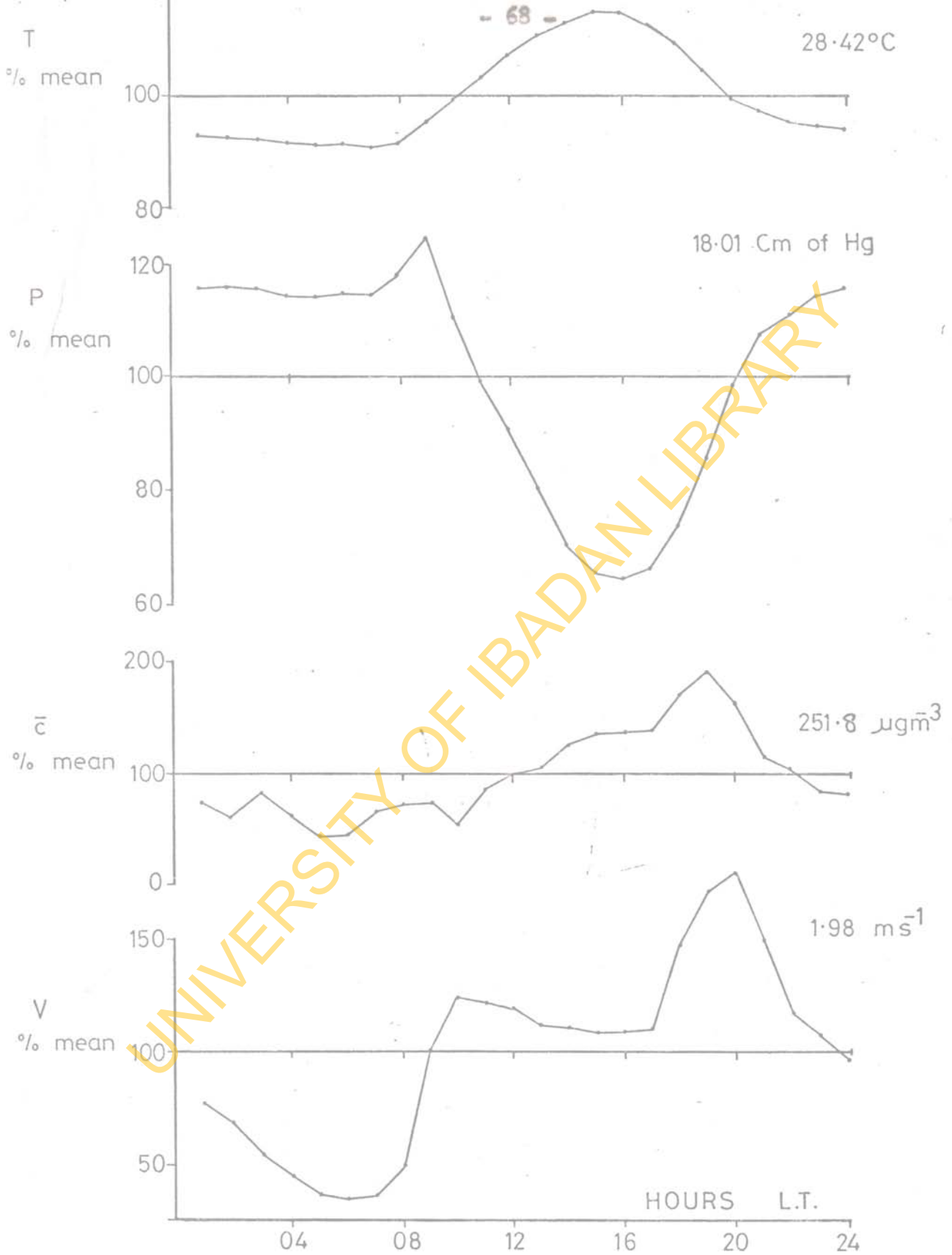
Fig.17c. Diurnal variation of the meterological elements T P c̄ and V for February 1979.
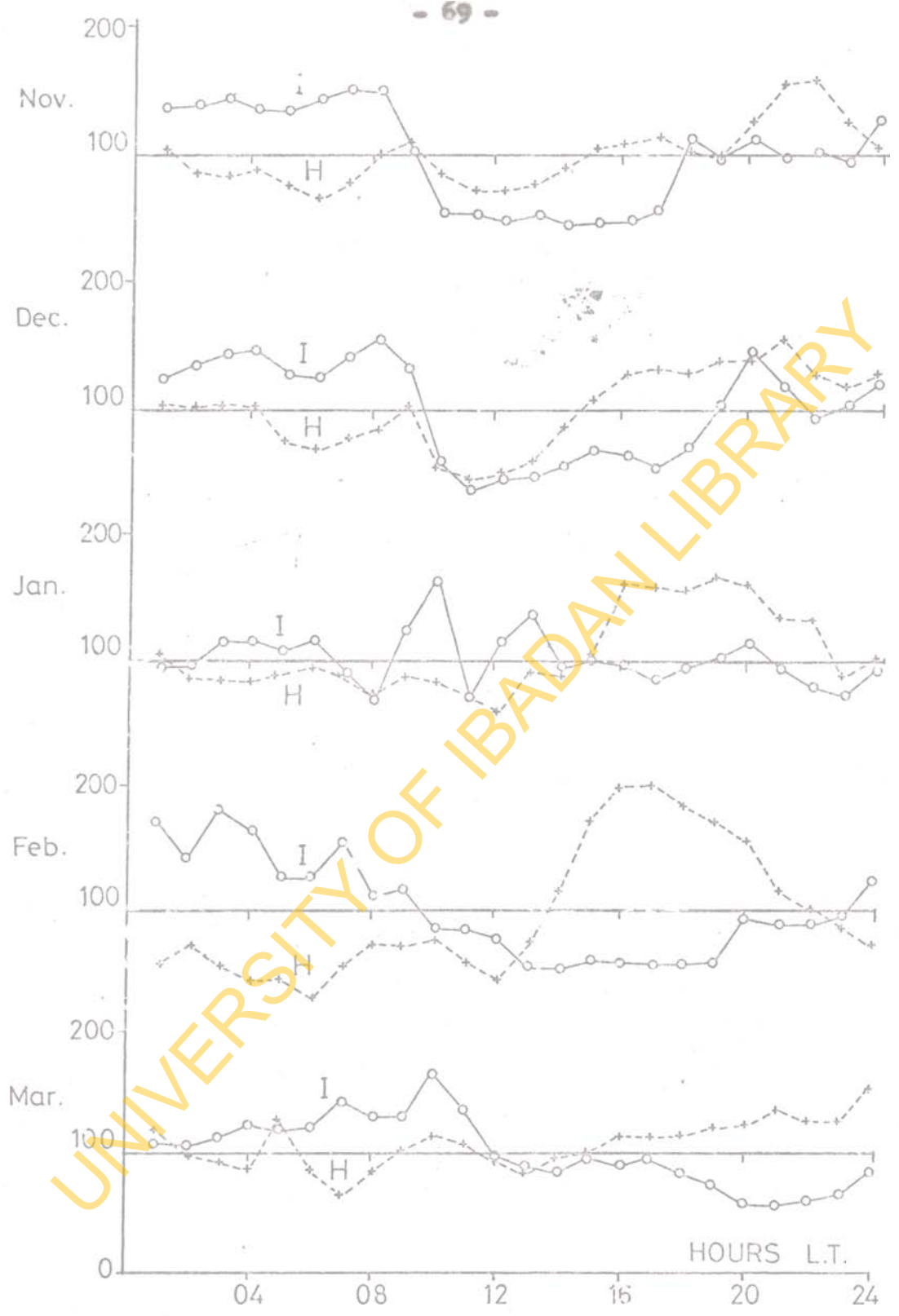
Fig.18a. Diurnal variations of H and I for Harmattan
Months of 1964

-o—o- I
-+···+- H
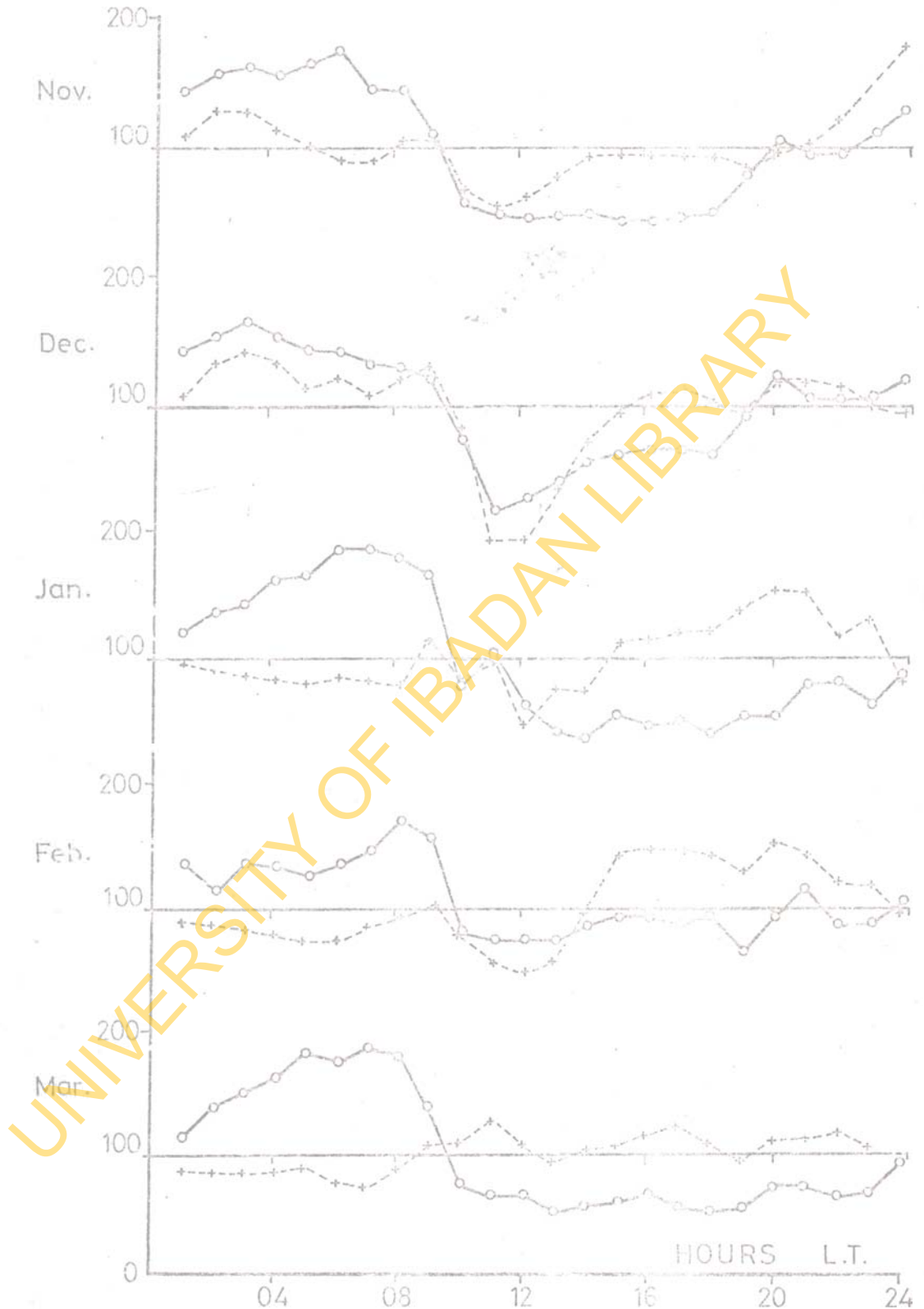
Fig.18b. Diurnal variations of H and I for the
Harmattan Months of 1965 .

    - o—o— I
    - +--+- H
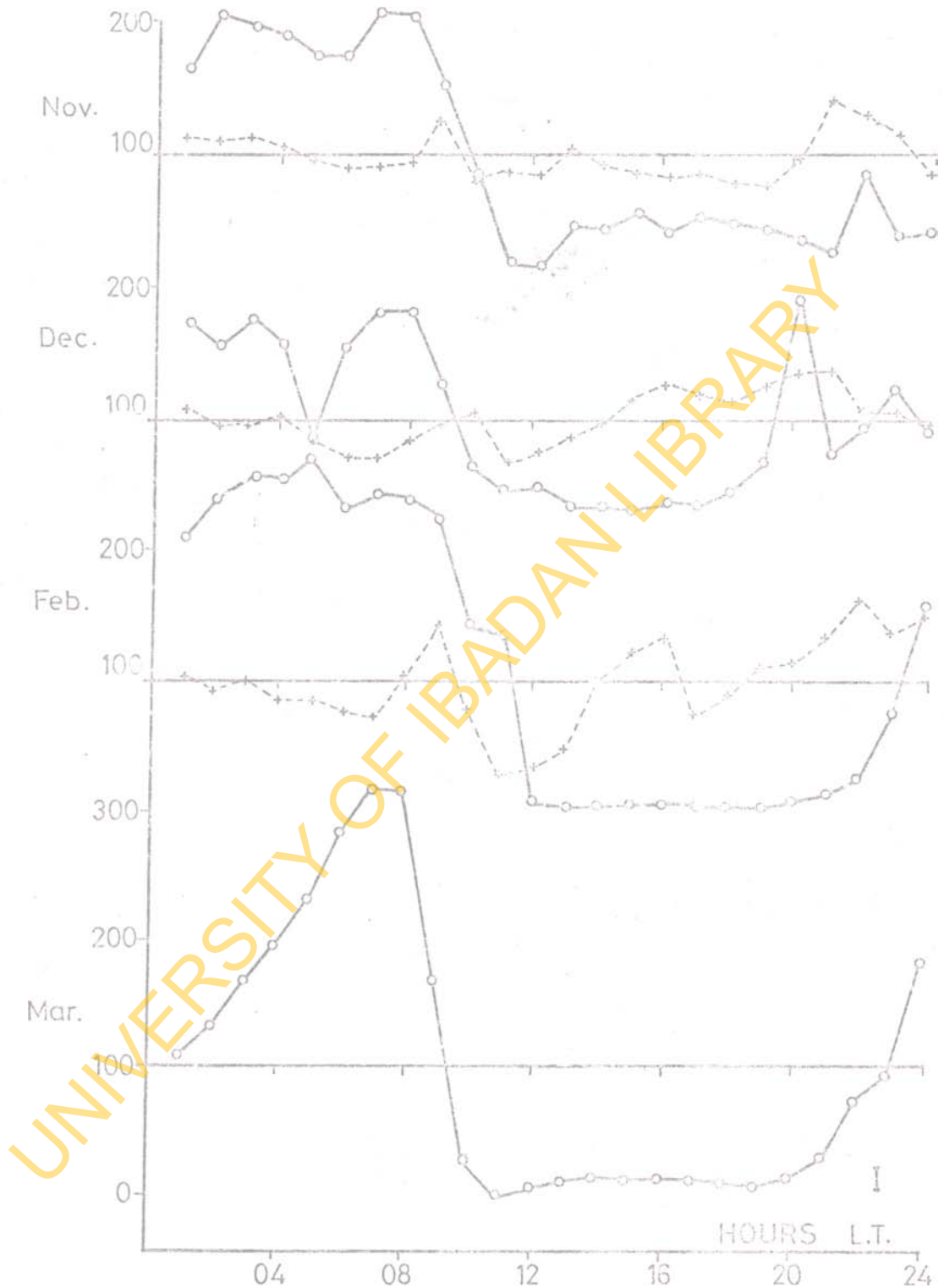
Fig.18c. Diurnal variations of H and I for the
Harmattan Months of 1968.

 —o—o—o I

 —+--+--+ H
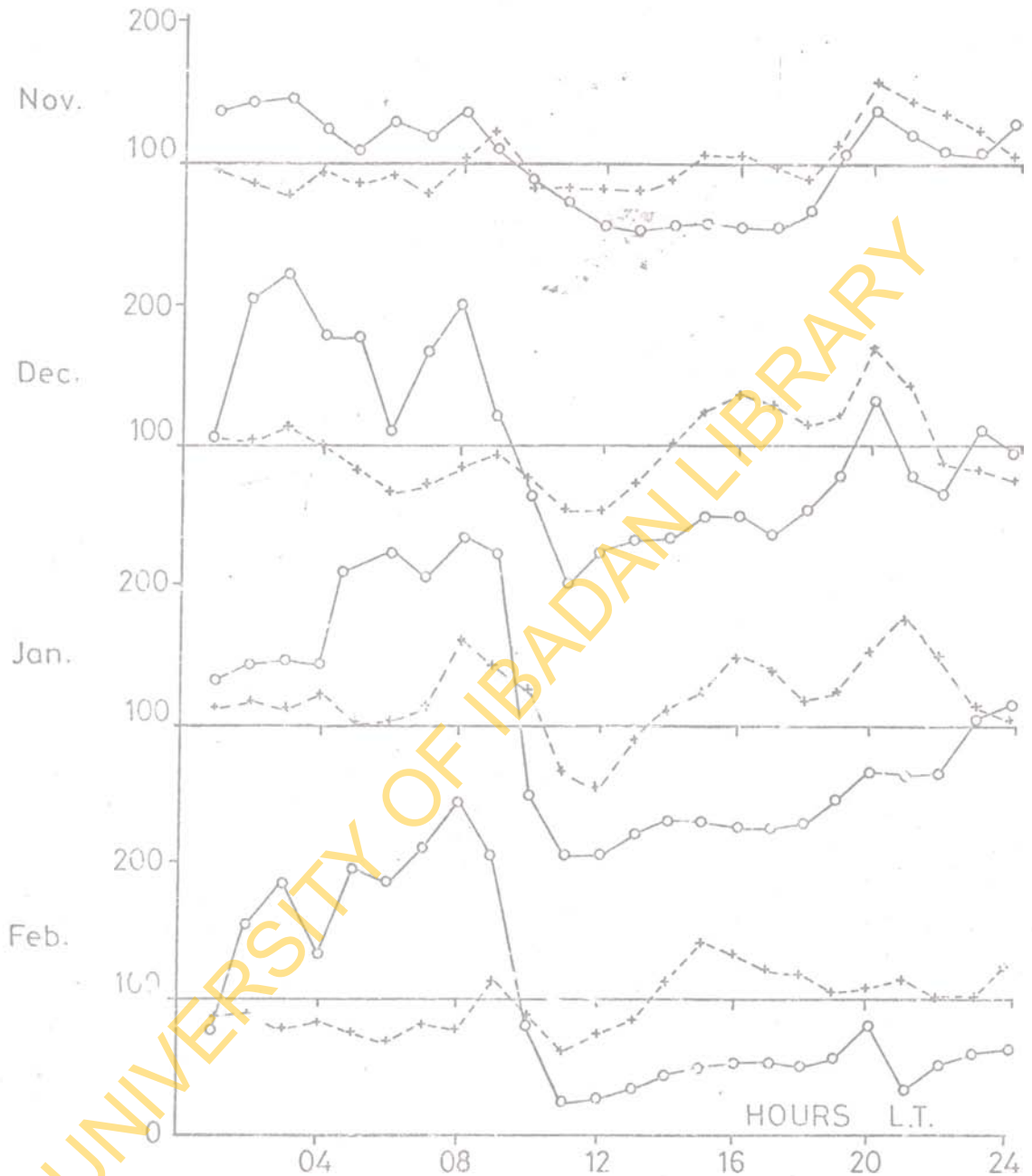
Fig. 18d.   Diurnal   Variations   of   H   and   I   during
Harmattan   Months   of   1969

—o—o—   I

--+--+--   H

during the current investigations.

3.1.2. <u>General Observations</u>: From the diurnal curves
obtained, from Fig 19 it will be observed that:

(i) The parameters I, λ, and ρ undergo similar diurnal
variations - single periodic with maximum in the morning and
very pronounced depressions during the "austausch" regime.
The parameters ρ and I often assume negative values during
the "austausch" regime.

It must be pointed out that the night values of the
conductivity are generally unreliable owing to frequent
insulation breakdowns due possibly to condensation. However,
for days on which reliable recordings were made, the
diurnal curves of I are generally similar to those depicted in
Figs 18 for the harmattan months of 1964, 1965, 1968 and 1969 for
this station.

(ii) The diurnal curves of vapour pressure follow a trend
fairly similar to those of the electrical parameters. (Figs. 18 & 19)

(iii) The dust concentration has a single periodic diurnal
variation - with a minimum between 0400 and 0800 hrs L.T.
and a maximum around 2000 hrs L.T. The observed trend is
roughly similar to the variation of wind speed.
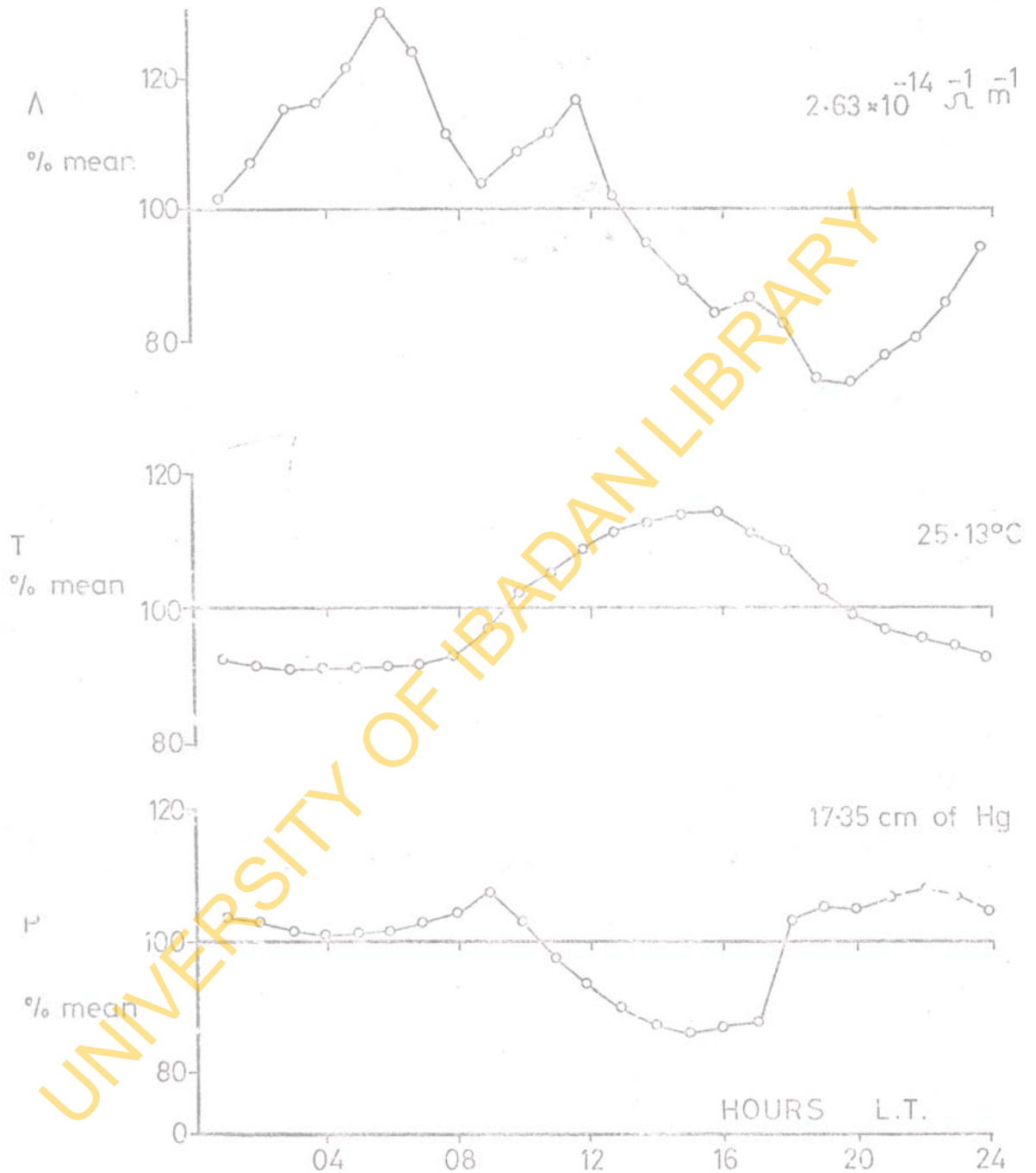
Fig.19a. Diurnal variations of Λ, T and P for November 1978.
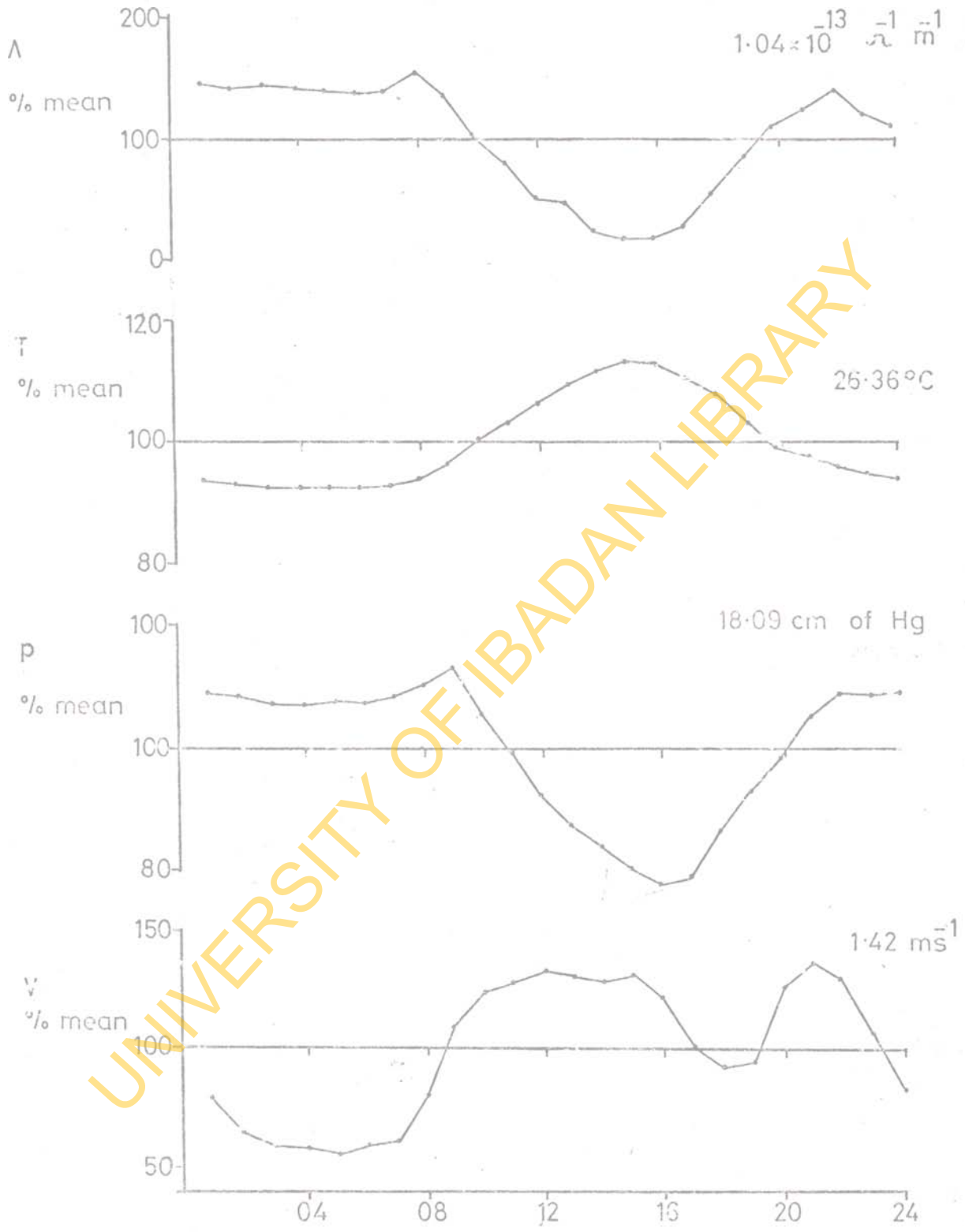
Fig. 19b. Diurnal variations of Λ, T, P and V for December 1978.
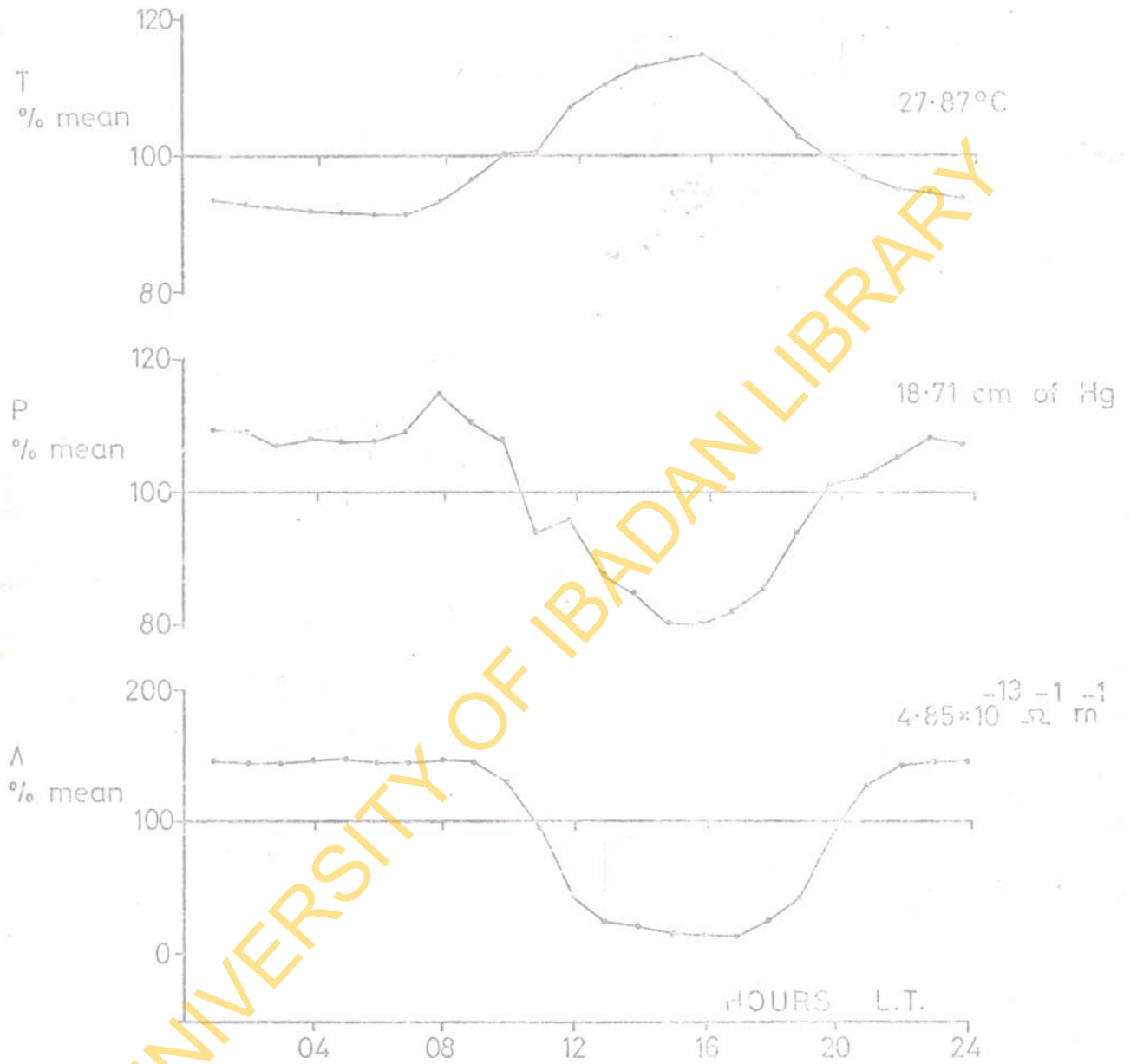
Fig. 19c. Diurnal variations of T, P and Λ for March 1979.
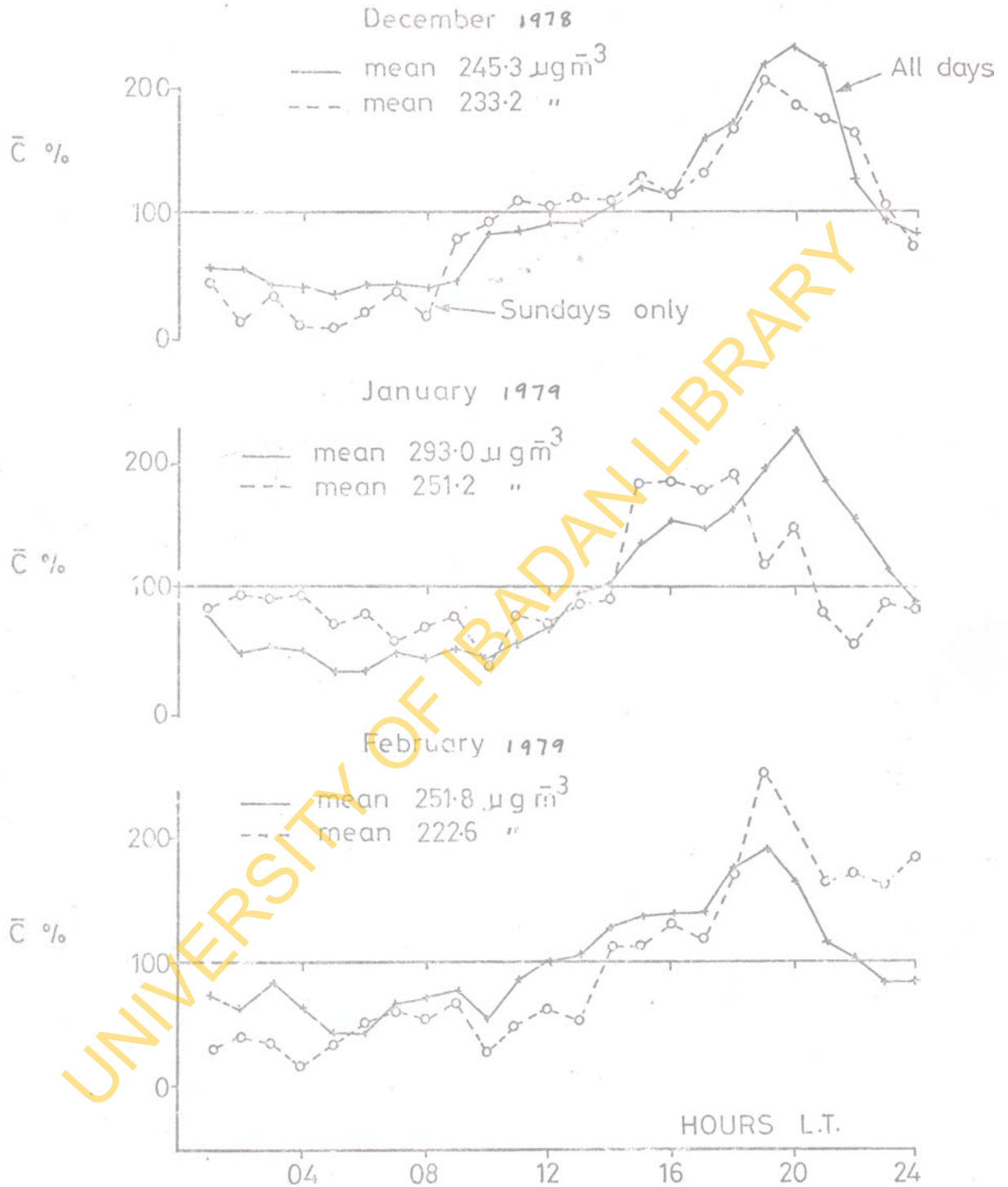
Fig. 20.   Dust   concentration   for   week days
and   for   Sundays   only.

(iv) The diurnal curves of I   exhibit peaks
at 0800 hrs L.T. Similar sharp increases have been observed
elsewhere (Ogawa 1960, Law 1963); and are also discernible
in some of the earlier curves of H and I (Fig. 18) for this
station.

(v) The severity of the harmattan - as measured by the
magnitude of the dust concentration in the atmosphere - is greatest i
January (See Fig 21). A similar observation has been made by
Oluwafemi (1978) from measurements made in Lagos .
(Lat. $6^{o}25'N$, Long. $3^{o}27'E$).

3.2. <u>Explanations to Observations</u>

The sharp maximum around 0800 hrs L.T. in electric
parameters H, I, λ and ρ is attributable to the sunrise
effect. Various suggestions have been made to account for
the effect. (Chalmers 1957, Mühleisen 1956, and Law 1963).
Mühleisen (1956) relates the sharp rise in the electric
parameters to the fact that there may be some effect caused
by the rays of the sun on the parameters. The sunrise
effect may be related to the general human activities in the
morning when smoke from kitchens and dust from the surround-
ings increase the conductivity of the air and also the
electrical parameters of the atmosphere.

The diurnal variation of the dust concentration,
measured directly for the first time in this locality,

exhibits a single-periodic variation with a broad minimum
occuring between 0400 hrs and 0800 hrs L.T. This variation
may be attributed to the fact that unlike the situation at
other times of the year when the pollution is due mainly to
traffic and local commercial activity, the situation during
the harmattan season ensures a copious and continuous supply
of dust from the Sahara desert throughout the day. The
effect of this is that an 'austausch' depression around noon,
which is usually associated with limited supply is absent.

Mean dust concentration obtained here ($245.3 \mu gm^{-3}$ for
December 1978) using the β-ray absorption technique compares
favourably with the mean value of $210 \mu g \ m^{-3}$ for December 1971
extracted from data of direct measurements of dust concentra-
tion here at Ibadan by Sanni (1973). His measurements
spanning the period July 1966 to February 1967 revealed a
significant level of radioactivity in harmattan dust
particles.

"Reduced" ground level dust concentrations obtained by
Oluwafemi 1980 (personal communication) for Lagos from light
extinction parameters measured with a Votz Sunphotometer
however indicate lower values. Lagos, it may be noted is
some 150Km south of Ibadan.

3.2.1. <u>Effect of Local activity on dust-concentration:</u>

Part of the dust in the air during the harmattan is raised
from the ground through the action of vehicles on traffic.
To investigate the extent of this contribution the dust
concentrations for each month were compared with the concen-
trations on Sundays which are rest days during which the
traffic volume and industrial activity are normally low.
The data are displayed in Fig. 20 for November to December
1978 and January to February, 1979.

The absence of any significant difference in the
magnitude and pattern of the diurnal variation of dust
concentration between Sundays and all days of the month is
an indication that traffic plays no significant role in the
level of dust in the atmosphere.

This is attributable to the fact that during the
harmattan period here in Nigeria the dry N.E. trade winds
blow down considerable quantities of dust from the Sahara
desert so much so that the local contributions through
traffic and industrial activities during week days in the
parameter is not noticeable. In highly industrialised areas
like Germany where the aerological conditions are very
largely controlled by human activities Mühleisen (1953)
observed significant differences between week-end and work
day values of the potential gradient.
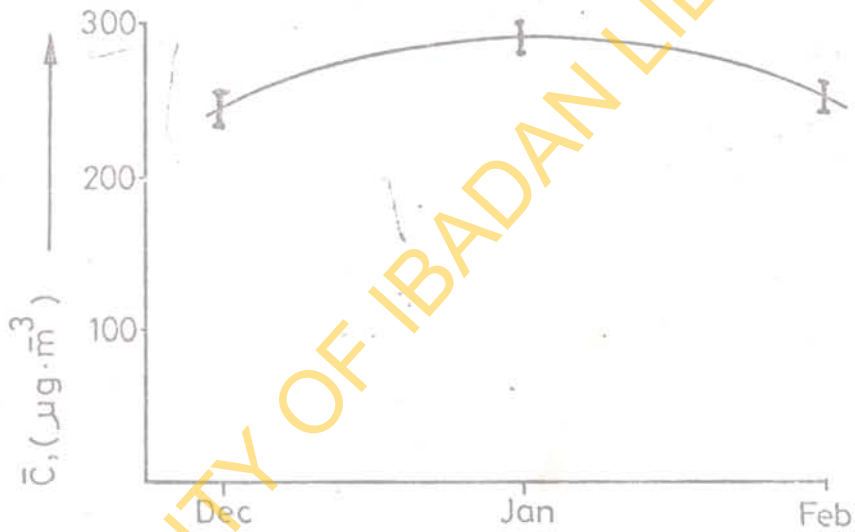
Fig.21. Mean dust concentrations
against the month for
Ibadan. (1978 to 1979)

3.2.2. Relation between dust concentration and conductivity:

During the harmattan season, fine dust particles blown south-
wards from the Sahara desert fill the air; and the
consequent charging of the particles through dispersal in
the prevailing dry atmosphere is bound to produce pronounced
effects on the polar conductivities. The conductivity may
therefore be expected to be closely related to the dust
concentration in the harmattan atmosphere. Attempts have
been made to exploit such a connection to monitor the dust
content in the Harmattan air-mass (Manes, 1977; Gringel and
Mühleisen, 1977) as well as in other types of air-mass (e.g.
Morita and Ishikawa, 1977) from measurements of the conducti-
vity. Since conductivity measurements can be made more
cheaply using ground based or baloon-borne sensors, the
advantages of this method of pollution monitoring are
obvious.

3.2.3. Theoretical Considerations: The basic ion-balance

equations for small ions in the atmosphere are (Chalmers 1967)

$$\frac{dn_1}{dt} = q - \alpha n_1 n_2 - \beta_{12} n_1 N_a - \beta_{10} n_1 N_c \quad - - - - (3.2)$$

and

$$\frac{dn_2}{dt} = q - \alpha n_1 n_2 - \beta_{21} n_2 N_1 - \beta_{20} n_2 N_0 \quad - - - - (3.3)$$

where n_1, n_2 are respectively the number of small +ve and -ve

ions per unit volume.

$N_1 N_2$ are respectively the number of large +ve and -ve

ions per unit volume

N_o = number of uncharged nuclei per unit volume.

q = the rate of production of small ions per unit

volume per second.

α = the recombination coefficient between small ions.

β_{12}, β_{21} = combination coefficient between small ions of

one sign and large ions of opposite signs (the

first suffix referring to small ions and the

second to large ions of opposite sign).

β_{10}, β_{20} = combination coefficient between +ve and -ve large

ions respectively with neutral nuclei.

Assuming that $n_1 \simeq n_2 = n$, say

and $N_1 \simeq N_2 = N$,

equations (3.2) and (3.3) may be written as

$$\frac{dn}{dt} = q - \alpha n^2 - \beta nN , \quad - \quad - \quad - \quad - \quad - \quad - \quad - \quad - \quad (3.4)$$

where $\beta = \beta_{12} + \beta_{10} {}^{N_o}/_N.$

When equilibrium is attained $\frac{dn}{dt}$ = 0, and equation (3.4)

may be solved to yield

$$n = \frac{-\beta N + (\beta^2 N^2 + 4 \alpha q)^{1/2}}{2\alpha} . \quad - \quad - \quad - \quad - \quad - \quad (3.5)$$

Now the polar conductivity is determined largely by the small ion density in accordance with the relation

$$n = \frac{\lambda_{\pm}}{eK_{\pm}} \qquad \qquad - \quad - \quad - \quad - \quad - \quad (3.6)$$

where e = electron charge and

$K_{\pm}$ = average mobility for small positive or negative ions.

Thus eliminating n between (3.5) and (3.6) we get

$$N = \frac{1}{\beta} \left(\frac{q}{\lambda} \frac{eK}{\lambda} - \frac{\alpha\lambda}{eK} \right) \qquad - \quad - \quad - \quad - \quad - \quad - \quad (3.7)$$

Barklie (1956) found that $2.1 < N_0/N < 3$; and Z/N increases as Z increases (Israel Vol. I), Z being the total number of charged and uncharged particles. Hence taking the upper value of N_0/N as applicable to harmattan situations, we may assume like Manes (1977) that $Z/N = 5$

$$\text{Hence} \quad Z = \frac{5}{\beta} \left(\frac{q}{\lambda_{\pm}} \frac{eK_{\pm}}{} - \frac{\alpha\lambda_{\pm}}{eK_{\pm}} \right) \qquad - \quad - \quad - \quad - \quad - (3.8)$$

and the particulate mass concentration in the atmosphere becomes

$$C = \frac{4}{3} \pi \rho \int_{r_{min}}^{r_{max}} r^3 Z(r) dr$$

$$= \frac{\frac{4}{3}\pi\rho \int_{r_{min}}^{r_{max}} r^3 Z(r)dr \cdot \int_{r_{min}}^{r_{max}} Z(r)dr}{\int_{r_{min}}^{r_{max}} Z(r)dr} \; ;$$

$$= \frac{\frac{4}{3}\pi\rho \int_{r_{min}}^{r_{max}} r^3 Z(r)dr \cdot Z}{\int_{r_{min}}^{r_{max}} Z(r)dr} , \quad \text{—} \;\text{—}\;\text{—}\;\text{—}\;\text{—} \quad (3.9)$$

where r = the radius of a typical nucleus species.

Direct measurements of the size distribution function $Z(r)$ of nuclei in the atmosphere over the total size range are difficult and available data are scanty and largely unreliable. However, assuming Jung's (1956) empirical law, $Z(r) = Cr^{-4}$, equation (3.9) integrates to yield

$$\bar{C} = \frac{4\pi Z\rho \ln \frac{r_{max}}{r_{min}}}{r_{min}^{-3} - r_{max}^{-3}} . \quad \text{—} \;\text{—}\;\text{—}\;\text{—}\;\text{—} \quad (3.10)$$

Assuming that $r_{min} = 6 \times 10^{-8}$ m and $r_{max} = 6 \times 10^{-6}$ m; and taking $\rho = 2.6 \times 10^3$ Kg m^{-3}; value for silicates, a major constituents of harmattan dust, equation (3.10) yields

$$\bar{C} = (32.66 \times 10^{-9} Z)\mu g.m^{-3} . \quad \text{—} \;\text{—}\;\text{—}\;\text{—}\;\text{—} \quad (3.11)$$

Putting $\beta_{n1} = 0.76 \times 10^{-11} m^3 s^{-1}$

$\beta_{n2} = 0.96 \times 10^{-11} m^3 s^{-1}$ based on Barklie's (1956) data

$K_+ = 1.14 \times 10^{-4} m^2 V^{-1} s^{-1}$

$K_- = 1.25 \times 10^{-4} m^2 V^{-1} s^{-1}$ Mohnen (1977)

$\alpha = 1.6 \times 10^{-12} m^3 s^{-1}$ Chalmers (1967)

$e = 1.6 \times 10^{-19} C$

equation (3.8) gives

$$Z = (12.0 \times 10^{-12} q / \lambda_+ - 5.77 \times 10^{22} \lambda_+) \quad - - -(3.12)$$

or $Z = (13.2 \times 10^{-12} q / \lambda_- - 5.26 \times 10^{22} \lambda_-)$

and equation (3.11) gives

$$\bar{C} = \left(3.92 \times 10^{-19} q / \lambda_+ - 18.84 \times 10^{14} \lambda_+\right)$$
$$- - - - -(3.13)$$
or $\bar{C} = \left(4.31 \times 10^{-19} q / \lambda_- - 17.18 \times 10^{14} \lambda_-\right)$

In Fig. 22, values of the dust concentration $\bar{C}$ are plotted against the corresponding unipolar conductivities $\lambda_\pm$ for measurements during the "austausch" period of the harmattan months of 1978-79. Using equation (3.13), theoretical curves are shown for three assumed values of q. As the experimental points lie between the curves for $q = 6 \times 10^6$ and 3.5×10^7 ion pairs per m^3 per second, it may be inferred that the rate of ion production during the
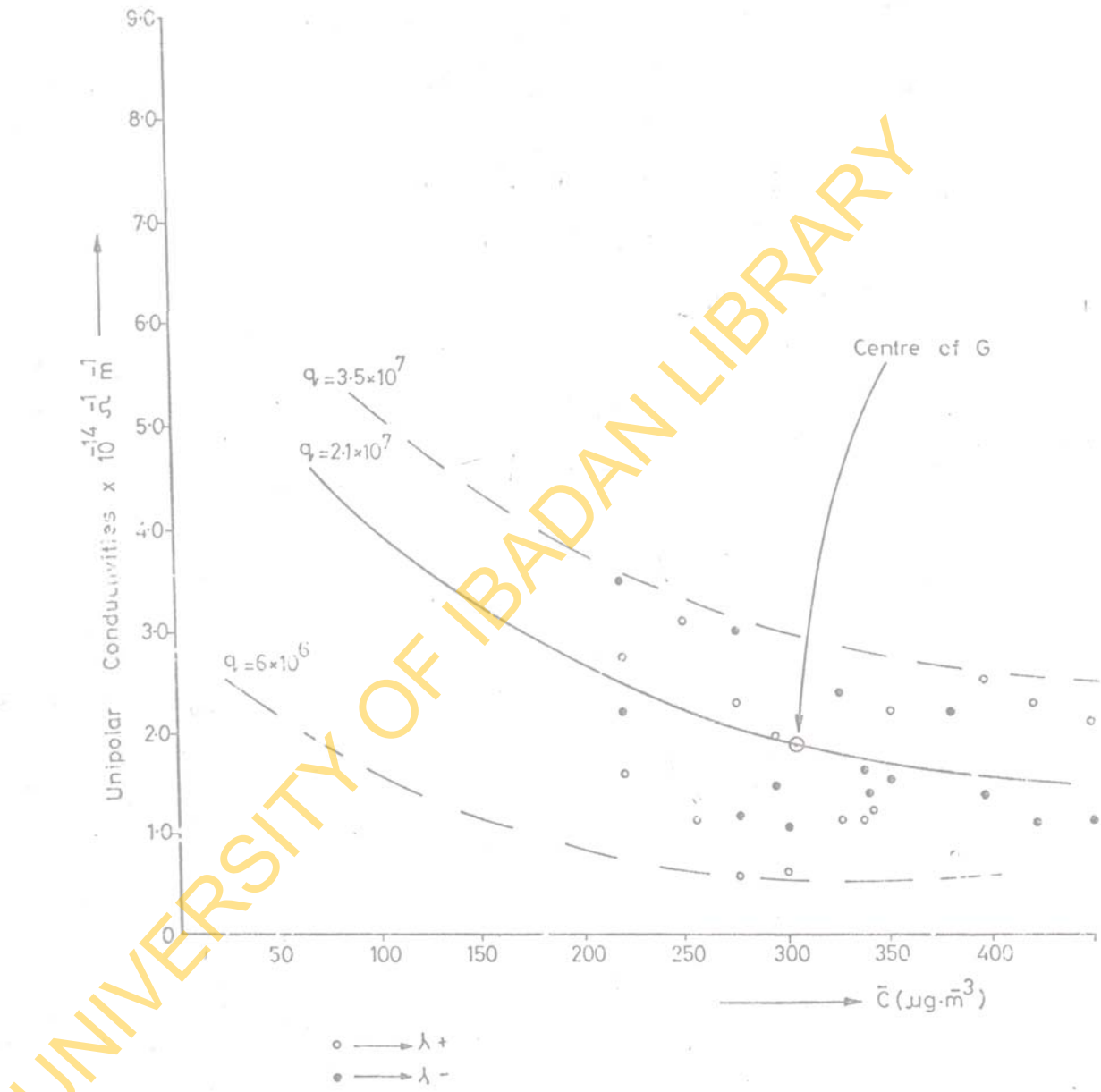
Fig. 22. Graph of Unipolar Conductivities against $\bar{C}$

harmattan season here in Ibadan lies between these two
values. The mean production rate of 2.1×10^{7} ion pairs
m^{-3} s^{-1} is chosen so that the middle curve divides the
plotted points more or less evenly.

It would be useful to obtain more data points for the
graph so that a more accurate theoretical relationship may
be obtained which could be used at similar locations where
the dust monitoring equipments are not available. On the
basis of the data so far collected it would appear that the
dust concentration here during the "austausch" regime may be
estimated from conductivity measurements using either the
relation

$$\bar{C} = 8.23 \times 10^{-12}/\lambda_{+} - 18.84 \times 10^{14}\lambda_{+} \text{ in } \mu g \ m^{-3}$$

$$\bar{C} = 9.05 \times 10^{-12}/\lambda_{-} - 17.18 \times 10^{14}\lambda_{-} \text{ in } \mu g \ m^{-3}$$

Substituting the mean value of q obtained above into
equation 3.12, estimates of Z can be obtained using the
measured values of λ_{+} or λ_{-}. For example, from the January
1979 data for λ_{+} we have that λ_{+} at 1600 hrs L.T. =
$2.12 \times 10^{-14}(\Omega m)^{-1}$, whence Z_{1600}hrs = 1.1×10^{10} particles
m^{-3}.

Another estimate of Z may be made if it is assumed that
the decrease in the conductivity around 1600 hrs is due
almost entirely to the presence in the atmosphere of aerosol
particles, while at night the effect of these particles may

be neglected. Following the procedure adopted by Gringel
and Mühleisen (1977) we may write, assuming equality of
concentration of ions of both signs and absence of aerosols
(e.g. at night)

$$\frac{dn_o}{dt} = 0 = q - \alpha n_o^2 \qquad \text{---} \quad \text{---} \quad \text{---} \quad \text{---} \quad (3.14)$$

where n_o = night-time concentration of ions of one sign.
During the day when the presence of aerosols hastens the
small ion depletion, we have; again assuming equality of
concentration of ions of both signs,

$$\frac{dn}{dt} = 0 = q - \alpha n^2 - \bar{\beta} n Z' \quad \text{---} \quad \text{---} \quad \text{---} \quad \text{---} \quad (3.15)$$

where

        n = day time concentration of ions of one sign

        $\bar{\beta}$ = effective attachment coefficient of ions on aerosol

           particles,

and Z' = No. of uncharged particles and half number of

           charged particles.

Putting $\triangle n = n_o - n,$ —   —   —   —   - (3.16)

we have, combining eqns (3.14), (3.15) and (3.16),

$$\bar{\beta} Z' = \triangle n . 2\alpha \left(1 + \frac{\triangle n}{2n}\right) \quad \text{---} \quad \text{---} \quad \text{---} \quad \text{---} \quad (3.17)$$

Now, $neK+ = \lambda+$, so that $\triangle n = \dfrac{\triangle \lambda+}{eK+}.$

Hence equation (3.17) yields

$$Z' = \frac{\triangle\lambda+ \cdot 2\alpha}{eK+\bar{\beta}}(1+\frac{\triangle\lambda+}{2\langle\lambda+\rangle})$$

where $\langle\lambda+\rangle$ = mean night value of $\lambda+$

$\triangle\lambda+$ = depression in $\lambda+$ at 1600 hrs below $\langle\lambda+\rangle$,

$\bar{\beta}$ = $\beta_{n_1}/5 = 1.5 \times 10^{-12} m^3 s^{-1}$

with $\langle\lambda+\rangle = 1.85 \times 10^{-13} (\Omega m)^{-1}$ and

$(\triangle\lambda+)_{1600 \text{ hrs}} = 1.64 \times 10^{-13} (\Omega m)^{-1}$, the equation

yields

$Z'_{1600 \text{ hrs}} = 2.76 \times 10^{10}$ particles m^{-3}.

Now, $Z' \simeq \frac{4}{5} Z$, and so the above value is about 20% low or 80% of $\bar{z}$

However, since the depression in the conductivity during "austausch" is not due entirely to the influx of aerosols, estimates based on the conductivity curve may be expected to be high. Assuming that on the average the two tendencies annul each other, we may accept the above numerical value as a fair measure of Z, the total nuclei concentration.

SUMMARY

The diurnal patterns of some electric and meteorological parameters are studied during five Harmattan months — November 1978 to March 1979 — in Ibadan.

The dust concentration (measured with a Philips Model PW 9790 dust minotor) and the polar conductivities (measured with a Gerdien capacitor of local construction) are investigated routinely in this locality for the first time, though values of the dust concentration here may be deduced from the data of Sanni (1973) who sampled the air for radioactivity.

The parameters like vapour pressure, air-earth current density, space-charge density and conductivity, which are controlled largely by local conditions, exhibit pronounced 'arstausch depressions' associated with vertical exchange of Physical properties. This is in agreement with the results obtained by Ette and Oluwafemi.

On the other hand the dust concentration, which is controlled during the Harmattan season largely by sources situated well outside the locality, exhibits a single periodic variation with a minimum between 0400 and 0800 hurs L.T. and a maximum at 2000 hrs L.T.

Using well-known relations between dust concentration and polar conductivity it has been possible to estimate.

(a) the average number density of dust particles during the 'austausch regime' to be 1.1×10^{10} particles m^{-3};

(b) the average small ion production rate as 2.1×10^{7} ion pairs $m^{-3} s^{-1}$.

SUGGESTION FOR FURTHER WORK

It will be useful to repeat the above study, with the number density of particles and the size distribution of the dust particles sampled directly.

REFERENCES

Barklie (1956) Quoted from Chalmers.(1967)

Beccaria,G.B. (1775) Quoted from Chalmers, (1967)

Bent,R.B. (1964) The testing of apparatus for ground fair - weather space - charge measurements J. Atmosph. Terr. Phys. 26, 313-318

Bhartendu (1969) The atmospheric electric potential gradient variation at land stations. Arch. Met. Geoph. Biokl. A. 18 pp. 345-363.

Chalmers, J.A. (1957) Effects of condensation nuclei in atmospheric electricity. Geof. Pur. Appl. 36, 211-17

Chalmers, J.A. (1967) 'Atmospheric Electricity' 2nd Edition Pergamon Press

Dolezalek, H. (1972) Discussion of the fundamental problem of atmospheric electricity. Pure Appl. Geophys. 100, 8-43

Ette, A.I.I. (1966) Ph.D. Thesis London University.

Ette, A.I.I. (1972) An effect of space charge advection on vertical air-earth current measurements. Arch. Met. Geoph. Biokl A 21 329-338

Ette, A.I.I. and Utah, E.U. (1973) Studies of point-discharge characteristics in the atmosphere. J. Atmosph. Terr. Phys. 35, 1799-1809

Gish, O.H. (1951) Universal aspects of atmospheric electricity. In: " compendium of meteorology" 101-119

Halmilton, R.A. and J.W. Archibold. Meteorology of Nigeria and Adjacent Territory Quart. J.R. Met. Soc. 71, 231-265.

Israel, H. (1948) Quoted from Israel, H (1950)

Israel, H " The atmospheric electric field and its meteorological causes" In: Thunderstorm electricity (eds. H.R. Byers pp 4-23. University of Chicago Press, 1950

Israel, H and P. de Bruijn (1967) " The present status of atmospheric electric Research." Arch. Met. Geoph. Biokl. A 16 H. 4 pp 282 - 300

Jung   (1956)   Quoted from Mohnen (1977)

Kasemir,H.W.   (1950)   Quoted from Chalmers (1967)

Kasemir,H.W.   (1955)   Measurement of the air - earth current
                                  density. Wentworth Conf. pp 91-95

Kelvin, Lord   (1960)   Atmospheric electricity, Roy Instn.
                                  lect: Elect. and Mag. pp 208-26

Law, J.   (1963)   The ionisation of the atmosphere
                                  near the ground in fair weather.
                                  Quart. J.R. Met. Soc. 89, 107-121

Lemomier L.G.   (1952)   Quoted from Chalmers, 1967

Lobodin, T.V.   (1968)   " On thunderstorm theory of Atmospheric
                                  electricity." IVth Int. Conf. on Atm.
                                  Elect. Tokyo.

Manes, A   (1977)   Particulate air pollution trends deduced
                                  from atmospheric electrical conductivity
                                  measurements at Bet-Dagan (Isreal) in
                                  " Electrical Processes in Atmospheres"
                                  (eds Dolezalek and Reiter).
                                  Steinkopff - Darmstadt

McKeown, H.D.J.   (1958)   Dust concentrations in the Harmattan
                                  Quart. J.R. Met. Soc. 84, 280-282

Mohnen, V.A.   (1977)   Formation, Nature and Mobility of ions
                                  of atmospheric importance in " Electical
                                  processes in atmospheres" (eds. H.
                                  Dolezatek and R. Reiter) 1-16. Steinkopff
                                  - Darmstadt.

Morita,Y and   (1977)   On recent measurements of electric para-
Ishikawa, H.   meters and aerosols in oceanic atmosphere
                                  in " Electrical processes in Atmospheres"
                                  (eds H. Dolezalek and R. Reiter)
                                  pp 126-130. Steinkopff - Darmstadt.

Muhleisen,R   (1956)   "On the deviations of the course of
                                  elements of atmospheric electricity on
                                  continents from the world wide course.
                                  J. Atmosph. Terr. Phys. 8, 146 - 157

Muhleisen,R   (1971)   New determination of the air - earth
                                  current over the ocean and measurement
                                  of ionospheric potentials.
                                  Pure Appl. Geophs., 84, 112-117

Ogawa, T.   (1960)   Diurnal variation in atmospheric
                                          electricity . . . . . .
                                          J. Geomagn. Geoelect. Kyoto 12, 1-12.

Oluwafemi, C.O.   (1971)   Ph.D. Thesis Ibadan University.

Oluwafemi, C.O.   (1978)   Measurements of spectral aerosol
                                          extinctions and precipitable water in
                                          Lagos during a Harmattan season.
                                          Pre-WAMEX symposium on meteorology and
                                          climatology of the West African Monsoon,
                                          Ibadan.

Sanni, A.O.   (1973)   Seasonal variation of atmospheric
                                          radioactivity at Ibadan.
                                          Tellus xxv, 80-85

Watson, W.   (1951)   Phil Trans. 47, 362

Webb, W.C.   (1971)   " Global Electrical Currents'
                                          Pure Appl. Geophys. 84, 89-106

Whipple, F.J.W.   (1929)   Potential gradient and atmospheric
                                          pollution: The influence of summer
                                          time.
                                          Quart. J. Ray. Met. Soc. 55, 351-361

Whipple, F.J.W. and (1936)   Point discharge in the electric field
Scarse, F.J.   of the earth.
                                          Geophs. Mem, Lond. 68, 1-20

Whilson C.T.T.   (1920)   "Investigations on lightning discharges
                                          and on the electric field of thunder-
                                          storms." Phil. Trans. A 221 73-115.

Table 2: <u>Saturation Vapour Pressure of Water</u> (1_s) <u>as a</u>
<u>Function of Temperature</u>

	Temp. in °F	S.V.P. in Cm. of Mercury		Temp. in °F	S.V.P. in Cm. of Mercury
				80	26.0
				81	27.0
	52	9.8		82	28.0
	53	9.9		83	28.7
50°	54	10.5	80°	84	28.7
	55	11.0		85	30.6
	56	11.4		86	31.7
	57	11.8		87	32.6
	58	12.3		88	33.7
	59	12.8		89	34.7
	60	13.3		90	35.9
	61	13.7		91	37.1
	62	14.2		92	38.2
	63	14.7		93	39.6
60°	64	15.3	90°	94	40.7
	65	15.8		95	42.0
	66	16.3		96	43.2
	67	16.9		97	44.6
	68	17.5		98	46.2
	69	18.1		99	47.5
	70	18.8		100	49.0
	71	19.6			
	72	20.0			
	73	20.8			
70°	74	21.4			
	75	22.1			
	76	22.8			
	77	23.7			
	78	24.3			
	79	25.2			

Vapour pressure p = R.H. (as a fraction) x
Sat. vapour pressure of water at the
relevant temp. $(1_s)_T$

i.e. p = R.H. x $(1_s)_T$

Appendix 2

1-3. SPECIFICATIONS (Measured at 25°C).

DC VOLTAGE GAIN, OPEN LOOP:
  Unloaded: Greater than 20,000.
  1000-ohm load: Greater than 12,000.

INPUT CHARACTERISTICS:
  Resistance: Greater than 10^{14} ohms.
  Capacitance: Less than 10 picofarads.
  Current Offset: Less than 5×10^{-14} ampere.
    Drift: Less than 10^{-15} ampere/24 hours.
    Temperature Coefficient; Less than 10^{-15} ampere/°C.
  Voltage Offset: Adjustable to zero.
    Drift: Less than 500 microvolts/hour averaged over any 24-hour period after two-
    hour warm-up.*
    Temperature Coefficient: Less than 500 microvolts/°C.*
  Input Voltage Noise:
    (0.1-10 cps): Less than 5 microvolts rms.
    (10 cps-100 kc): Less than 5 millivolts rms.
  Current Noise (0.1-10 cps): Less than 5×10^{-15} ampere peak-to-peak.
  Overload Limit: ± 400 volts.**

FREQUENCY CHARACTERISTICS:
  Closed Loop Unity Gain, Small Signal: dc to 100 kc (-3db).
  Slewing Rate: 1 volt/microsecond minimum.
  Gain Bandwidth Product: Greater than 150 kc.
  Rolloff: Approximately 6 db/octave.

OUTPUT:
  Amplifier: ± 11 volts at 11 milliamperes.
  Reference Voltage: +13.5 volts at 1 milliampere, regulated to $\pm 0.1\%$ for 10% change in
  input.

OPERATING TEMPERATURE: 0 to 50°C

CONNECTORS: Input: push-on coaxial receptacle, Amphenol 2175. All other connections:
15-terminal 1/16 inch card-edge.

POWER REQUIREMENTS:
  +16 to +25 volts unregulated, 35 milliamperes plus output current;
  -16 to -25 volts unregulated, 8 milliamperes plus output current.
  Note: Model 300 will also operate to specifications with standard 15-volt $\pm 0.1\%$
    regulated power supplies.

DIMENSIONS, WEIGHT: 3-1/2 inches high x 4 inches wide x 1-1/2 inches deep; net weight,
13 ounces.

ACCESSORIES SUPPLIED: Mating card-edge connector and Teflon-insulated coaxial input
connector with shield (chassis mounting).

----

*With 100% feedback this drift as a percent of full output is less than 0.005%/hour (or/°C,
**With a 10^5 ohm or greater feedback resistor without a shunting capacitor. May require
several hours to recover to specified drift with severe overload.

Appendix 3

TABLE 3. Models 301 and 301K Specifications.

Specifications measured at 25°C.	MODELS 301 AND 301K
DC VOLTAGE GAIN, OPEN LOOP:	
Unloaded (Minimum)	50,000
Full Load (Minimum)	30,000
INPUT CHARACTERISTICS:	
Common Mode	
Resistance (Minimum)*	5×10^{12} ohms
Shunt Capacitance (Maximum)	10 picofarads
Rejection (Minimum)	60 db
Voltage Limit	± 11 volts
Between Inputs	
Resistance (Minimum)	10^{12} ohms
Shunt Capacitance (Maximum)	10 picofarads
Overload Limit	± 400 volts continuous either input to ground or between inputs
Current Stability	
Offset	10^{-14} ampere
vs. Time (worst case)	10^{-15} ampere/24 hours
vs. Temperature (worst case)	Doubles every 5°C
vs. Supply (worst case)	10^{-15} ampere/% (301K)
Voltage Stability	
Offset	Adjustable to zero
vs. Time (worst case)	2 millivolts/week after 1-hour warm-up
vs. Temperature (worst case)	150 microvolts/°C
vs. Supply (worst case)	300 microvolts/% (301K)
Current Noise	
0.1-10 cps (Maximum peak-to-peak)	5×10^{-15} ampere
Voltage Noise	
0.1-10 cps (Maximum rms)	10 microvolts
10 cps—500 kc (Maximum rms)	100 microvolts
FREQUENCY:	
Gain Bandwidth Product (Minimum)	500 kc
Slewing Rate (Minimum)	0.3 volt/microsecond
Rolloff (Nominal)	6 db/octave
OUTPUT:	
Amplifier	± 11 volts @ 11 milliamperes
Reference Voltage	± 15 volts @ 5 milliamperes (301)
Regulation	$\pm 1.0\%$ for 10% input change (301)
OPERATING TEMPERATURE:	$-25°C$ to $+85°C$
CONNECTORS:	
Input	2 Push-on Teflon-insulated coaxial
All Other	15 terminal 1/16" card edge
POWER REQUIREMENTS:	
Voltage (positive and negative)	19 to 30 v unreg., 2 v p-p max. ripple (301); 15 v reg. $\pm 0.1\%$ (301 & 301K)
+Current (Plus output current)	16 ma (301); 5 ma (301K)
—Current (Plus output current)	16 ma (301); 5 ma (301K)
DIMENSIONS; WEIGHT:	3½" high x 4" wide x 1½" deep; 13 ounces
ACCESSORIES SUPPLIED:	Mating card-edge connector and 2 push-on coaxial connectors

*5×10^{12} ohms minimum from -11 to +5 volts common mode decreasing to 10^{12} minimum at +11 volts common mode.